# A REINVESTIGATION OF THE KINETICS AND MECHANISM OF LIGAND EXCHANGE IN μ-(2,2,8,8-TETRAMETHYL-3,7-DITHIANONANE)-DECACARBONYLDITUNGSTEN(0)

THESIS

Presented to the Graduate Council of the
University of North Texas in Partial
Fulfillment of the Requirements

For the Degree of

MASTER OF SCIENCE

By

Jing-Piin Liao, B.S.
Denton, Texas

August, 1988

Liao, Jing-Piin, A Reinvestigation of the Kinetics and Mechanism of Ligand Exchange in μ-(2,2,8,8-tetramethyl-3,7-dithianonane)decacarbonylditungsten(0). Master of Science (Chemistry), August, 1988, 77 pp., 7 tables, 26 illustrations, bibliography, 25 titles.

The substitution reaction of $W_2(CO)_{10}(\mu\text{-DTN})$ (DTN = 2,2,8,8-tetramethyl-3,7-dithianonane) with $P(OCH(CH_3)_2)_3$ is stepwise. The kinetics of step 1 and step 2 follow the rate laws :

$$-d[(DTN)W_2(CO)_{10}]/dt = \frac{k_{1d}k_2[\text{ligand}][(DTN)W_2(CO)_{10}]}{k_{-1}[(DTN)W(CO)_5] + K_2[\text{ligand}]}$$

and

$$-d[(DTN)W(CO)_5]/dt = \frac{k_{2d}k_3[\text{ligand}][(DTN)W(CO)_5]}{k_{-2}[DTN] + k_3[\text{ligand}]} .$$

The plots of $k_{obsd}$ (for step 1) versus [ligand] and $k'_{obsd}$ (for step 2) versus [ligand] are hyperbolic curves, and the plots of $1/k_{obsd}$ verse 1/[L] and $1/k'_{obsd}$ versus 1/[L] exhibit linear behavior.

Because both coordinated DTN as $(DTN)W(CO)_5$ and the DTN ligand remain close to $W(CO)_5$ after dissociation, the values

of the competition ratios $k_{-1}/k_2$ and $k_{-3}/k_4$, which range from 14.9 to 25.6, are larger than those obtained from others' experiments.

ACKNOWLEDGEMENT

I would like to acknowledge my uncle, Mr. Lin Feng-Chou, for his encouragement to come to the United States to continue my education. I would like to thank my family, especially for their love, understanding and financial support of my studies. Lastly and most importantly I would like to thank my father, who just recently passed away. I dedicate this work to his memory.

TABLE OF CONTENTS

LIST OF TABLES

LIST OF ILLUSTRATIONS

# CHAPTER I

## INTRODUCTION

A thorough appreciation of the chemistry of the transition metals requires a knowledge of their reaction mechanisms. Kinetic and mechanistic studies of octahedral carbonyls and their derivatives can provide an understanding of factors which influence ligand substitution processes in metal carbonyls. An investigation of ligand displacement reactivity requires a brief consideration of the bonding between metal and carbonyls. Sidgwick (1) and Mitchell and Parish (2) have already suggested the "eighteen electron rule" for the rationalization of the stoichiometries and structures of the transition metal complexes, particularly carbonyls and organometallic compounds. Based on their theory, transition metal complexes in which the valence shell of the metal atom has eighteen electrons have greater stability than those with less or more valence electrons.

The most important energetic component of the bonding in transition metal complexes is ligand-to-metal $\sigma$ donation. Since, however, the back-bonding component assumes greater relative importance when the metal has many electrons to dissipate, low oxidation states are stablized by $\pi$-acid ligands(3). The bonding of carbon monoxide, CO, to a metal is called a $\pi$-acid ligand bond. It can be seen from the

valence bond structure of carbon monoxide :C≡O: that the electron pair on the carbon atom is available for donation to the metal due to the smaller value of the electronegativity of the carbon atom relative to that of the oxygen atom. The molecular orbital diagram shown in Figure 1 indicates that there is a non-bonding $\sigma$-electron pair (HOMO) located on C and empty $\pi^*$ orbitals (LUMOs) of the carbon monoxide; therefore, the bonding between carbon monoxide and the central metal atom results from the overlap of the filled C orbital and an empty metal sigma orbital as shown in Figure 2-A, and the $\pi$-back-bonding may be ascribed to the overlap of the empty $\pi^*$ orbitals of CO and filled metallic orbitals as shown in Figure 2-B.

Both types of bonding reinforce each other (3) : back-bonding increases the effective nuclear charge of the metal and restrains the metal-to-carbonyl donation of electrons while increasing the carbonyl-to-metal donation of electrons; at the same time, the movement of electrons from carbonyl to metal diminishes the effective nuclear charge of the metal, and makes the metal-to-carbonyl electron flow possible. For these reasons, carbon monoxide forms a very large number of complexes with transition metals in low oxidation states, even though CO is an extremely poor sigma donor.

This synergic bonding has been examined in many ways. The most striking evidence for back-bonding in transition metal carbonyls is the reduction in the carbon-oxygen stretching or

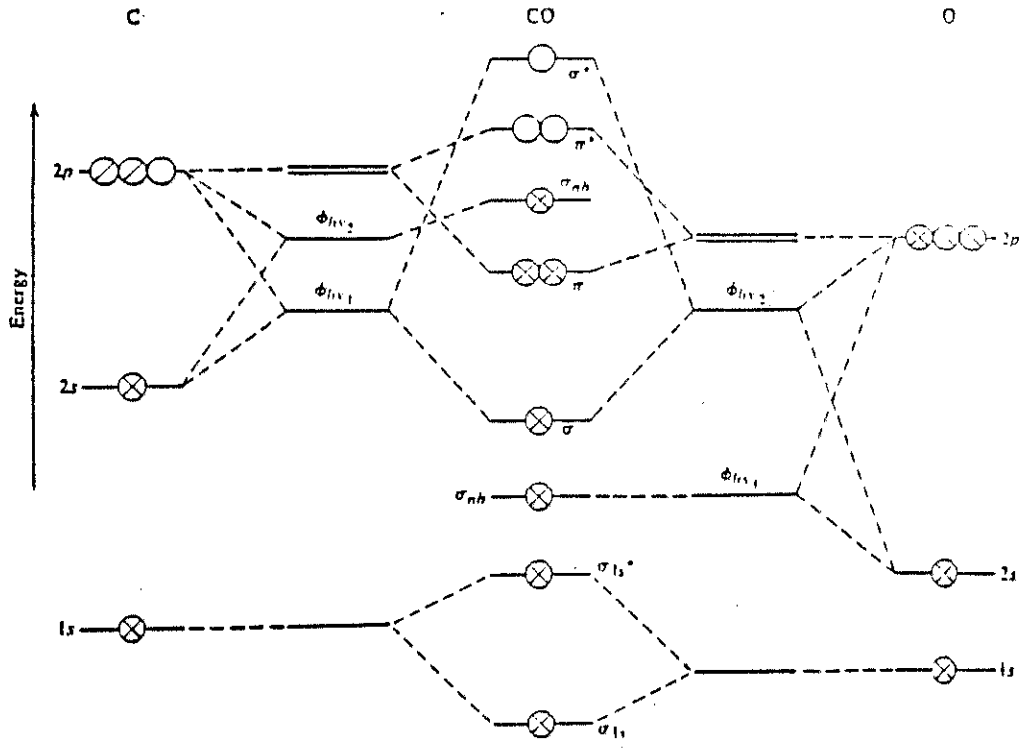


Figure 1. The molecular orbital energy-level diagram for CO. Adapted from M. Orchin and H. H. Jaffe, Symmetry, Orbitals and Spectra, Wiley-Interscience, New York, 1971, p. 47.

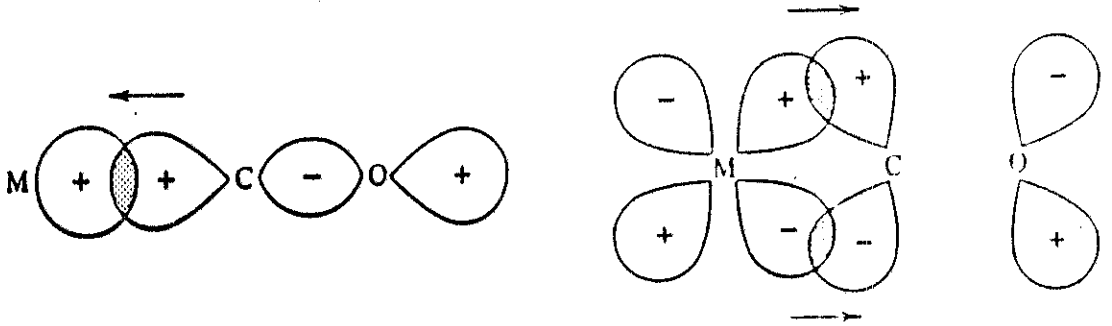


*(a)* Ligand-to-metal σ-bonding

*(b)* Metal to ligand $\pi^*$ back bonding (one of a mutually perpendicular set shown)

Figure 2. Orbital overlap in M-CO bonding. Adapted from B. Douglas, D. McDaniel and J. J. Alexander, Concepts and Models of Inorganic Chemistry 2nd edition, John Wiley & Sons, Inc. New York, 1983, p. 406.

force constant compared to that of free carbon monoxide (4). Thus, a higher metal-carbonyl bond order is implied by a lower frequency V(CO) and force constant Fe(CO). The carbon-oxygen stretching frequency in transition metal carbonyls is in the range of 2200-1800 $cm^{-1}$ in the infrared spectral region. From the CO stretching modes, information about the molecular structure can be obtained. The numbers and intensities of the bands depend largely on the local symmetry about the central metal atom to which the carbonyls are attached. Using distinct CO stretching frequencies in infrared spectroscopy for metal carbonyl complexes, reaction products can be monitored and the purity of the complexes can be determined (5).

Models of Ligand Substitution Processes. Of primary interest are ligand substitution reactions of transition metal carbonyl complexes. This type of reaction involves the breaking of metal-ligand bonds and the formation of new bonds. The substitution ligand, a Lewis base, can replace either the substituent S as shown in equation 1-1 or a carbonyl as shown in equation 1-2:

$$M(CO)_x(S)_y + L' \longrightarrow M(CO)_x(S)_{y-1}L' + S \quad \text{----------(1-1)}$$

$$\text{or} \quad M(CO)_x(S)_y + L' \longrightarrow M(CO)_{x-1}(S)_yL' + CO \quad \text{-----(1-2)}$$

In any attempt to investigate the substitution reactions of transition metal carbonyl complexes in a systematic manner,

classification of these substitution reactions into types of reaction pathways is necessary. These reactions are divided into three main categories: (I) the dissociative, D, mechanism, (II) the associative, A, mechanism, (III) the dissociative interchange, $I_d$, and associative interchange, $I_a$, mechanisms (3, 11).

For the D mechanism, one elementary step is detectable as shown in equation 1-3: the complex collects enough energy through irreversible processes to break the M-X bond as shown in equation 1-3; then this five-coordinate complex reacts rapidly with Y to form the product as shown in equation 1-4.

$$L_5MX \xrightarrow{k_1} L_5M + X \text{ ----------(1-3)}$$

$$L_5M + Y \xrightarrow{\text{fast}} L_5MY \text{ ----------(1-4)}$$

The rate law, which is first order, is expressed as:

$$- d[L_5MX]/dt = k_1[L_5MX] \text{ ----------(1-5)}$$

Angelici and Basolo (6) studied the reactions of $Mn(CO)_5Z$ ( Z = F, Br, Cl ) with different ligands such as CO, $PR_3$, $AsR_3$ and aniline (Figure 3), all of which were determined to have the same rate constant for a given Z. Kinetics data showed that the rates of reaction depend neither on the nature of Y nor its concentration. As a result, these reactions are

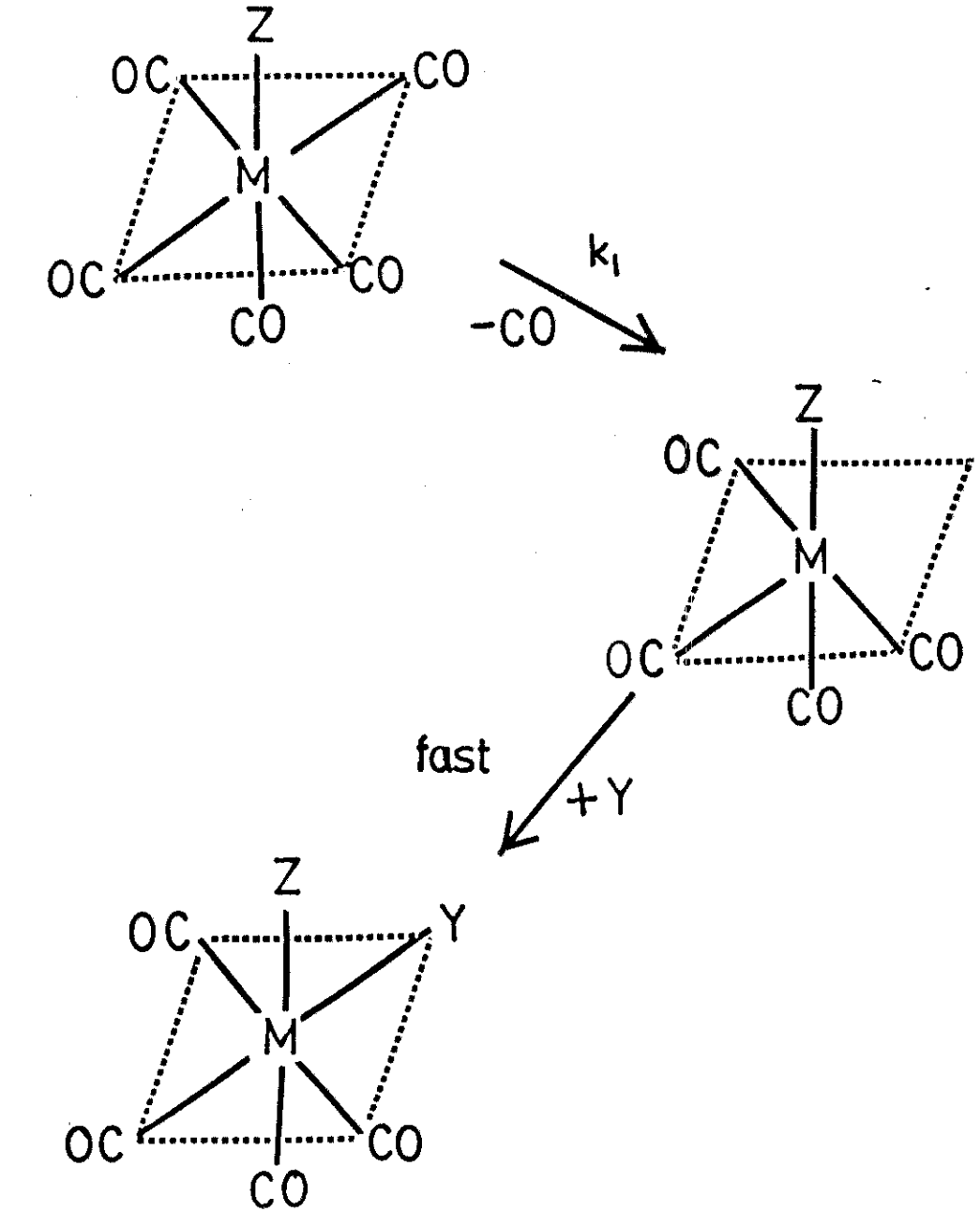


Figure 3. Substitution reaction mechanism involving rate-determining dissociation of carbon monoxide.

assigned a simple dissociative mechanism.

For the more complex D mechanism, two elementary steps are detected: the complex accumulates enough energy through a reversible process to break completely the M-X bond, leaving a five-coordinate intermediate as shown in equation 1-6; then, this steady-state intermediate reacts with Y (which could be a solvent) in the second coordination sphere as shown in equation 1-7 (3).

$$L_5MX \underset{k_{-1}}{\overset{k_1}{\rightleftharpoons}} L_5M + X \text{ ----------(1-6)}$$

$$L_5M + Y \xrightarrow{k_2} L_5MY \text{ ----------(1-7)}$$

In terms of experimentally-measurable concentrations, the rate law, which is pseudo first order, becomes

$$-\frac{d[L_5MX]}{dt} = \frac{k_1k_2[Y][L_5MX]}{k_{-1}[X] + k_2[Y]} \text{ --------(1-8)}$$

which can reduce to

$$-\frac{d[L_5MX]}{dt} = k_1[L_5MX] \text{ ----------(1-9)}$$

When $k_2[Y] >> k_{-1}[X]$. This limiting rate law as shown in equation 1-9 is the same as that of the simple D mechanism as

shown in equation 1-5. Detection of the intermediate provides proof for this reversible process D pathway (7).

In one possible A mechanism, the ligand attacks the central atom of the complex to form a seven-coordinate intermediate, as shown in Figure 4. Another possibility is that the reaction takes place by attack at the carbonyl carbon, as shown in Figure 5.

Under the condition that bond-making to an entering group is the main factor determining the size of the activation energy, and an intermediate of higher coodination number (seven-coordinate) survives long enough to be detected, the reactions are assigned the associative mechanism as shown in equation 1-10 and 1-11 (3, 8) .

$$L_5MX + Y \underset{k_{-1}}{\overset{k_1}{\rightleftharpoons}} L_5MXY \text{----------(1-10)}$$

$$L_5MXY \xrightarrow{k_2} L_5MY + X \text{----------(1-11)}$$

The rate law is expressed as :

$$-\frac{d[L_5MX]}{dt} = \frac{k_1[L_5MX][Y]}{k_{-1} + k_2} = k_3[L_5MX][Y] \text{ -----(1-12)}$$

here , $k_3 = \dfrac{k_1}{k_{-1} + k_2}$

Although no firmly established examples of mechanism 1-10 and 1-11 have been observed for octahedral substitution

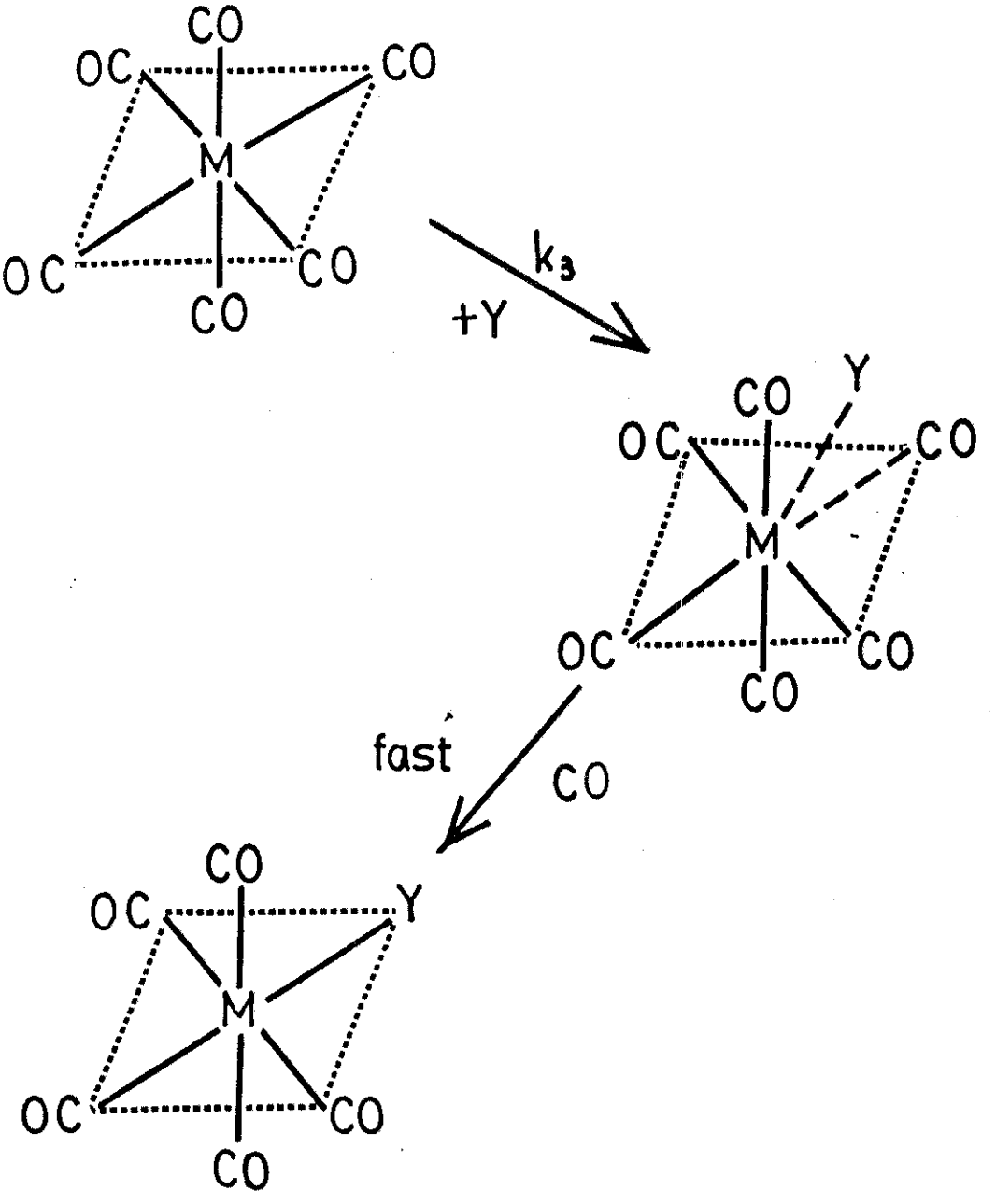


Figure 4. Substitution reaction mechanism involving rate-determining attack of Y ligand at the metal atom.

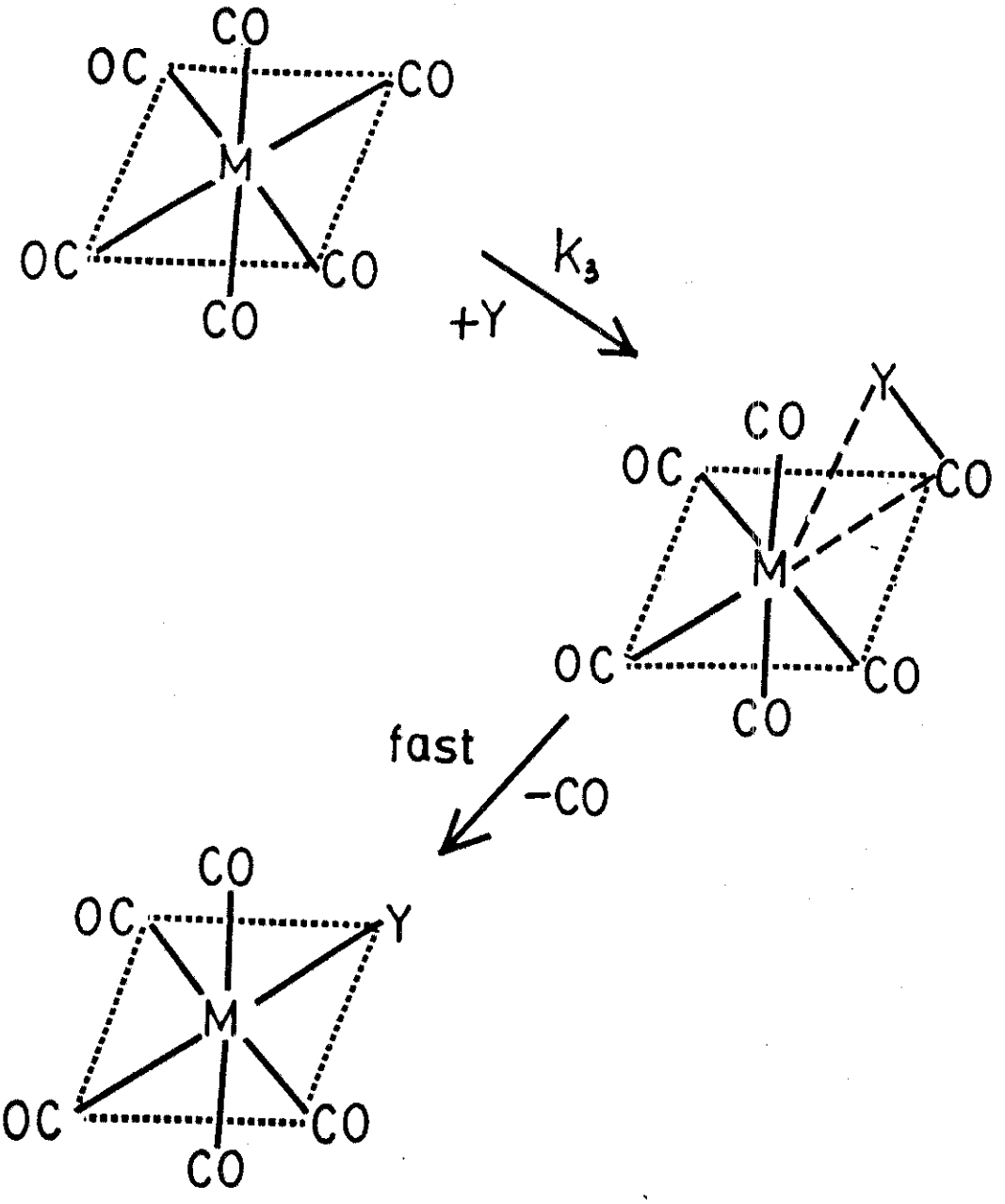


Figure 5. Substitution reaction mechanism involving rate-determining attack of Y ligand at the carbonyl carbon.

reactions (3), the reactions of tungsten and molybdenum hexacarbonyls with tetrabutylammonium halides are believed to proceed through formation of a seven-coordinate intermediate by attack of the halide at the carbonyl carbon in step 1-10 (9). The structure of these reaction products, $N(C_2H_5)_4^+[M(CO)_5NCO]^-$, strongly supports that the azide anion attacks the carbonyl carbon in the rate-determining step. Molecular orbital calculations which indicate a positive charge on the carbonyl carbon atoms in $Cr(CO)_6$ (10), and the absence of formation of azide compound $Cr(CO)_5N_3^-$, support this mechanism (4).

For dissociative and associative interchange mechanisms of the third type, $L_5MX$ accumulates sufficient thermal energy into the M-X vibration to begin to break the M-X bond. Before the bond can be broken fully, M begins to form a bond with any species Y, which could be a solvent molecule (11), which happens to be in a suitable position to enter the first coordination sphere (3). Also involved is the equilibrium constant for the outer sphere complex formation. This possible mechanism can be written as follows:

$$L_5MX + Y \overset{K}{\rightleftharpoons} (L_5MX,\ Y) \qquad \text{------(1-13)}$$

$$(L_5MX,\ Y) \xrightarrow{k} (L_5MY,\ X) \qquad \text{--------(1-14)}$$

$$(L_5MY,\ X) \xrightarrow{\text{fast}} L_5MY + X \qquad \text{----------(1-15)}$$

The experimental parameter most accessible is the initial concentration of the reactant complex $[L_5MX]_0$, which is

$$[L_5MX]_0 = [L_5MX] + [(L_5MX, Y)]$$
$$= [L_5MX] + K [L_5MX] [Y] \text{ ----------(1-16)}$$

then, $$[L_5MX] = \frac{[L_5MX]_0}{1 + K[Y]}$$

and the rate law is expressed as,

$$-\frac{d[L_5MX]}{dt} = \frac{kK[L_5MX]_0[Y]}{1 + K[Y]} \text{ ----------(1-17)}$$

For dissociative ($I_d$) and associative ($I_a$) interchange, both the entering and leaving groups are bound to the metal in the transition state. The difference between these two mechanisms is that in the $I_d$ mechanism, the extent of bond-breaking exceeds that of bond making; in the $I_a$ mechanism, it is the opposite, and the magnitude of k is controlled by the energy of bond formation (3).

The reaction of (amine)$Mo(CO)_5$ complexes with various nucleophiles investigated by Covey and Brown (12) has indicated that the "associative pathway" is best described as a dissociative interchange ($I_d$) process in which there is relatively little bond formation in the transition state.

In addition to these three main types of mechanisms, there

exists a two-term mechanism. It is a combination of the first type and the second type, and indicates a competition between first and second order reactions. The rate law for this mechanism is:

$$-d[L_5MX]/dt = k_1[L_5MX] + k_3[Y][L_5MX] \text{ -------(1-18)}$$

Most of the substitution reactions of transition metal carbonyl complexes obey this rate law. If the concentration of the ligand is in excess of 20-fold or greater than that of substrate $L_5MX$, the rate law of this two-term reaction can be expressed in terms of pseudo first order kinetics (8), as shown below:

$$-d[L_5MX]/dt = k_{obsd}[L_5MX] \text{ ----------(1-19)}$$

here $$k_{obsd} = k_1 + k_3[Y].$$

A plot of $k_{obsd}$ versus ligand concentration will exhibit linear behavior with a slope of $k_3$ and an intercept of $k_1$.

The reaction of metal hexacarbonyls with phosphites and phosphines studied by Angelici and Graham (13) has suggested the rate law:

$$-d[M(CO)_6]/dt = k_1[M(CO)_6] + k_3[Y][M(CO)_6] \text{ -------(1-20)}.$$

The second term is often of negligible importance. It

has been ascribed to either an associative process or a dissociative interchange (12).

The Problem. Dobson and Schultz have investigated the kinetics and mechanisms of ligand-exchange (2,2,7,7-tetramethyl-3,6-dithiaoctane)tetracarbonyltungsten(0) ((DTO)$W(CO)_4$) and in (2,2,8,8-tetramethyl-3,7-dithianonane) tetracarbonyltungsten(0) ((DTN)$W(CO)_4$) (14) (15), which supported a mechanism involving initial ring-opening and subsequent competing ring-reclosure and ligand attack at the ring-opened five coordinate intermediate. A new compound containing a bridging DTN ligand, $W_2(CO)_{10}$($\mu$-DTN) (DTN = 2,2,8,8-tetramethyl-3,7-dithianonane), was also synthesized (16).

The reaction of $\mu$-(2,2,8,8-tetramethyl-3,7-dithianonane)-decacarbonylditungsten(0) with triisopropyl phosphite in 1,2-dichloroethane was studied by Yang in 1982 (16). This study suggested a mechanism as shown in Figure 6 which included the dissociation of (DTN)$W(CO)_5$ from (DTN)$W_2(CO)_{10}$ for first step and dissociation of DTN from (DTN)$W(CO)_5$ for second step. The rate law for this reaction is expressed as:

$$k_{obsd} = k_{1d} + k_{1a}[L] \quad \text{----------(1-21)} \quad \text{for step 1}$$

and

$$k'_{obsd} = \frac{k_{2d}k_3[L]}{k_{-2}[DTN] + k_3[L]} \quad \text{-------(1-22)} \quad \text{for step 2.}$$

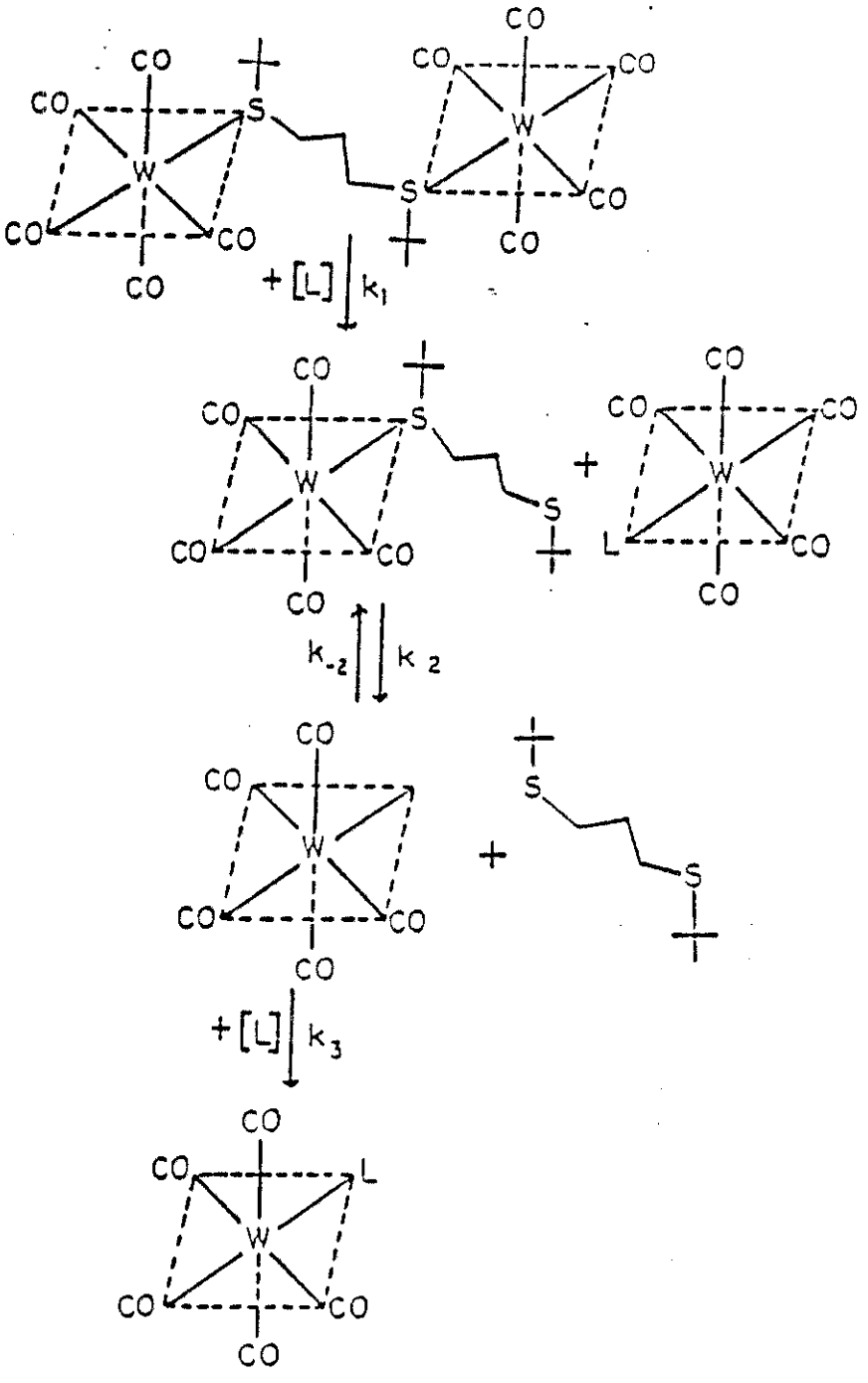


Figure 6. The mechanism of reaction of (DTN)$W_2(CO)_{10}$ with triisopropyl phosphite. Adapted from S. N. Yang's Thesis, Department of Chemistry, North Texas State University, Denton, TX 76203, 1982, p. 36.

Based on the above mechanism, the plots of $k_{obsd}$ values of step 1 versus ligand concentration show linear behavior. Therefore, $k_{1d}$ can be calculated from the intercept and $k_{1a}$ from the slope of the line in the plot of $k_{obsd}$ versus ligand concentration. For step 2, the plot of $k'_{obsd}$ versus ligand concentration exhibited nonlinear behavior, but the corresponding reciprocal plots of $1/k'_{obsd}$ versus $1/[L]$ were linear.

$$1/k'_{obsd} = 1/k_{2d} + k_{-2}[DTN]/k_{2d}k_3[L] \quad \text{-----(1-23)} \quad \text{for step 2.}$$

Thus $k_{2d}$ can be evaluated from the intercept in the plot of $1/k'_{obsd}$ versus $1/[L]$. Using the corresponding reciprocal equation, $1/k'_{obsd}$ versus $1/[L]$ results in a linear plot of slope $(1/k_{2d} \times k_{-2}[DTN]/k_3)$ and intercept $(1/k_{2d})$. Therefore $k_{-2}/k_3$ can be estimated as the value of slope/intercept obtained.

Yang found the value (16) of the competition ratios $k_{-2}/k_3$ to be about 12.5-14 . These values are too large when compared to the values of competition ratios obtained from other experiments such as those by Covey and Brown (12), Schutlz and Dobson (14), and Hyde and Darensbourg (17), all of which are near unity.

This student is interested in reinvestigating the kinetics and mechanism of the bridged compound in 1,2-dichloroethane with triisopropyl phosphite and in finding the reasons why the

values of competition ratio $k_{-2}/k_3$ in this reaction are so large.

## Chapter Bibliography


1. Sidgwick, N. V. The Chemical Elements and Their Compounds, Vols. I and II; Oxford Univ. Press: New York; 1950, 1703.

2. Mitchell, P. R.; Parish, R. V. J. Chem. Educ. 1969, 46, 811.

3. Douglas, B. E.; McDaniel and Alexander, J. J. Concepts and Models of Inorgnic Chemistry, 2nd. Ed. Jon Wiley & Sons, Inc. New York, 1983, 329-363 and 404-416.

4. Darensbourg, D. J.; Darensbourg, M. Y. Inorg. Chem. 1970, 9, 1691.

5. Angelici, R. J.; Malone, M. D. Inorg. Chem. 1967, 6, 1731.

6. Angelici, R. J.; Basolo, F. J. Am. Chem. Soc. 1962, 84, 2495.

7. Howell, J. A. S.; Burkinshaw, P. M. Chem. Rev. 1983, 83(5), 557.

8. Purcell, K. F.; Kotz, J. C. Inorganic Chemistry, W. B. Saunders; Philadelphia, PA.; 1979, 360-377.

9. Pardue, J. E.; Memering, M. N.; Dobson, G. R. J. Organometal. Chem. 1974, 71, 407.

10. Werner, H.; Beck, W.; Englemann, H. Inorg. Chim. Acta, 1969, 3, 331.

11. Langford, C. H.; Gray, H. B. Ligand Substitution Processes, W. A. Benjamin: New York, N.Y.; 1965, Chapter 1.

12. Covey, W. D.; Brown, T. L. Inorg. Chem. 1973, 12, 2820.

13. Graham, J. R.; Angelici, R. J. Inorg. Chem. 1967, 6, 2082.

14. Schultz, L. D.; Dobson, G. R. J. Organometal. Chem. 1976, 124, 19.

15. Dobson, G. R.; Schultz, L. D. J. Organometal. Chem. 1977, 131, 285.

16. Yang, S. N. "Kinetic Study of Ligand Exchange in

μ-(2,2,8,8-tetramethyl-3,7-dithianonane)decarbonyl-ditungsten(0)," 1982, Masters Thesis, North Texas State University.

17. Hyde, C. L.; Darensbourg, D. J. Inorg. Chem. 1973, 12, 1286.

# CHAPTER II

## EXPERIMENTS I & II

### Experiment I

Instruments for Thermal Reactions. The infrared spectra for identification of the substrate and product were obtained on a Nicolet 20SXB FTIR spectro- photometer. Reaction rates were monitored in the visible region on a Beckman Model DU-2 spectrophotometer. All samples for the kinetic experiments were weighed on a Mettler Balance, model H16, to 0.0001g. Kinetics data were analyzed by a linear least squares program on a Leading Edge computer.

Preparation and Purification of the Materials.

Triisopropyl Phosphite: $P(OCH(CH_3)_2)_3$ was purchased fromthe Aldrich Chemical Company. Sliced-sodium rinsed with hexane was added to $P(OCH(CH_3)_2)_3$ at about 5 % volume proportion, was kept under nitrogen for at least 24 hours, and then was fractionally distilled at 72-75 $^oC$ and 20 torr.

1.2-Dichloroethane: $C_2H_4Cl_2$ from the Aldrich Chemical Company was purified by reflux over phosphorus pentoxide for 8 h. It was then fractionally distilled at 83-84 $^oC$.

Tetrahydrofuran: $\overline{OCH_2CH_2CH_2CH_2}$ was purchased from the Matheson Coleman & Bell Company. It was refluxed over sodium and benzophenone for 12 h; then it was fractionally distilled at 66-67 $^oC$.

2,2,8,8-tetramethyl-3,7-dithianonane (DTN): One mole of sodium (23 g) was added to 500 mL of absolute ethanol in a one-liter, three-necked flask equipped with a mechanical stirrer, dropping funnel, reflux condenser and nitrogen inlet as shown in Figure 7. When the sodium was completely dissolved, one mole of t-butyl mercaptan (90 g) was slowly added through a dropping funnel. The reaction solution was then stirred for approximately 2 h. The flask was then cooled in a water/ice bath, and 1,3-dibromopropane (0.5 mol, 101 g) was added dropwise into the reaction mixture through the dropping funnel. The resulting mixture was then stirred under nitrogen for an additional hour at room temperature. Precipitated NaBr was removed by filtration. Ethanol was then removed from the filtrate under vacuum at 30 $^{o}$C and the residual DTN (liquid) was then purified by distillation under nitrogen at 168 $^{o}$C and 45 torr. The yield of DTN is in the range of 76 to 80 %, and its purity is approximately 98.85-99.25 % as determined by a Hewlett-Packed Model 5970A GC/MS system.

μ-(2,2,8,8-tetramethyl-3,7-dithianonane)decacarbonyl-ditungsten(0) ((DTN)W2(CO)10): Six g of $W(CO)_6$ were added to 220 mL of purified THF. This reaction mixture was photolysed for 2 h under nitrogen using a Hanovia 450-W medium pressure UV lamp in an immersion reactor as shown in Figure 8. The formation of the $(THF)W(CO)_5$ complex produced upon photolysis was checked by monitoring the IR spectrum at 2070 $cm^{-1}$ and 1940 $cm^{-1}$ until those absorbances reached their maximum

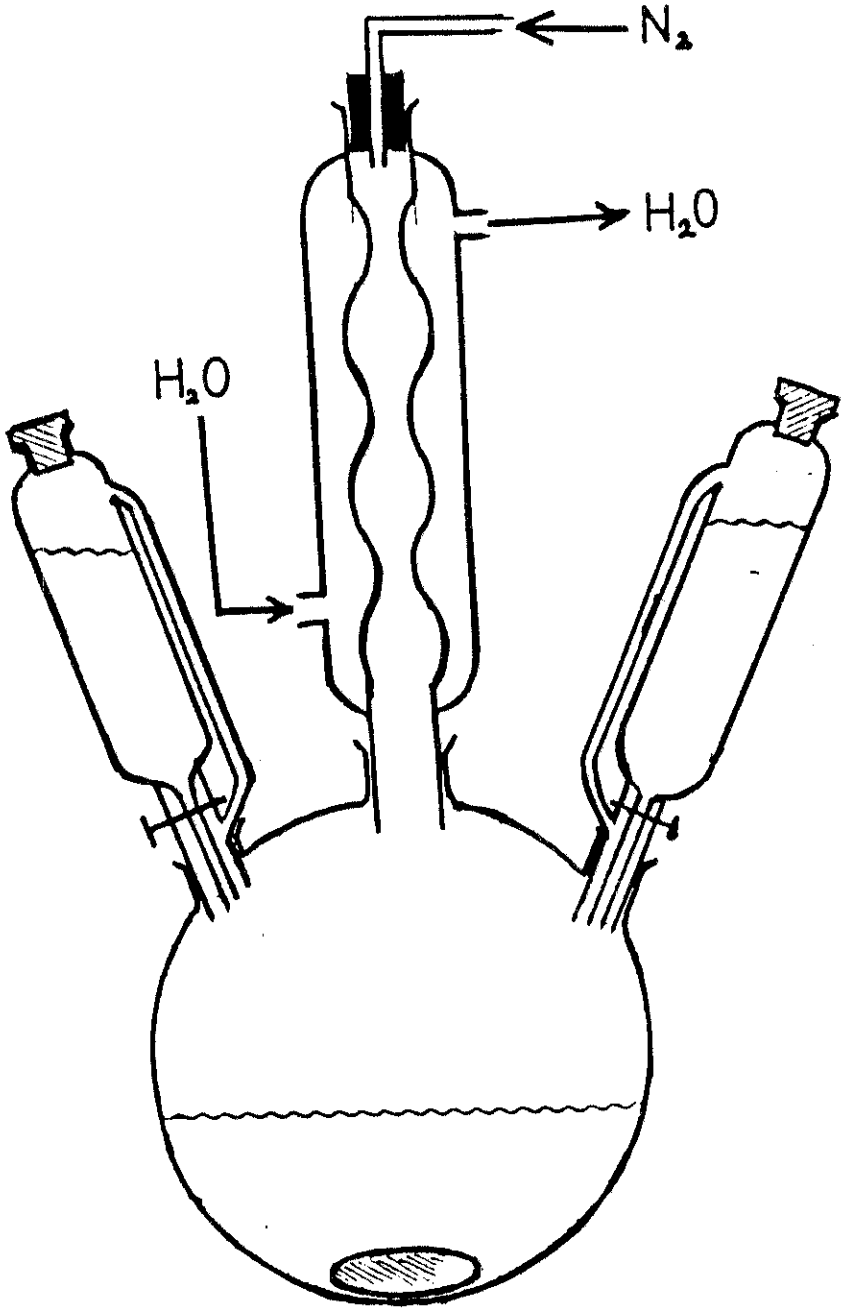


Figure 7. The apparatus for synthesizing DTN.

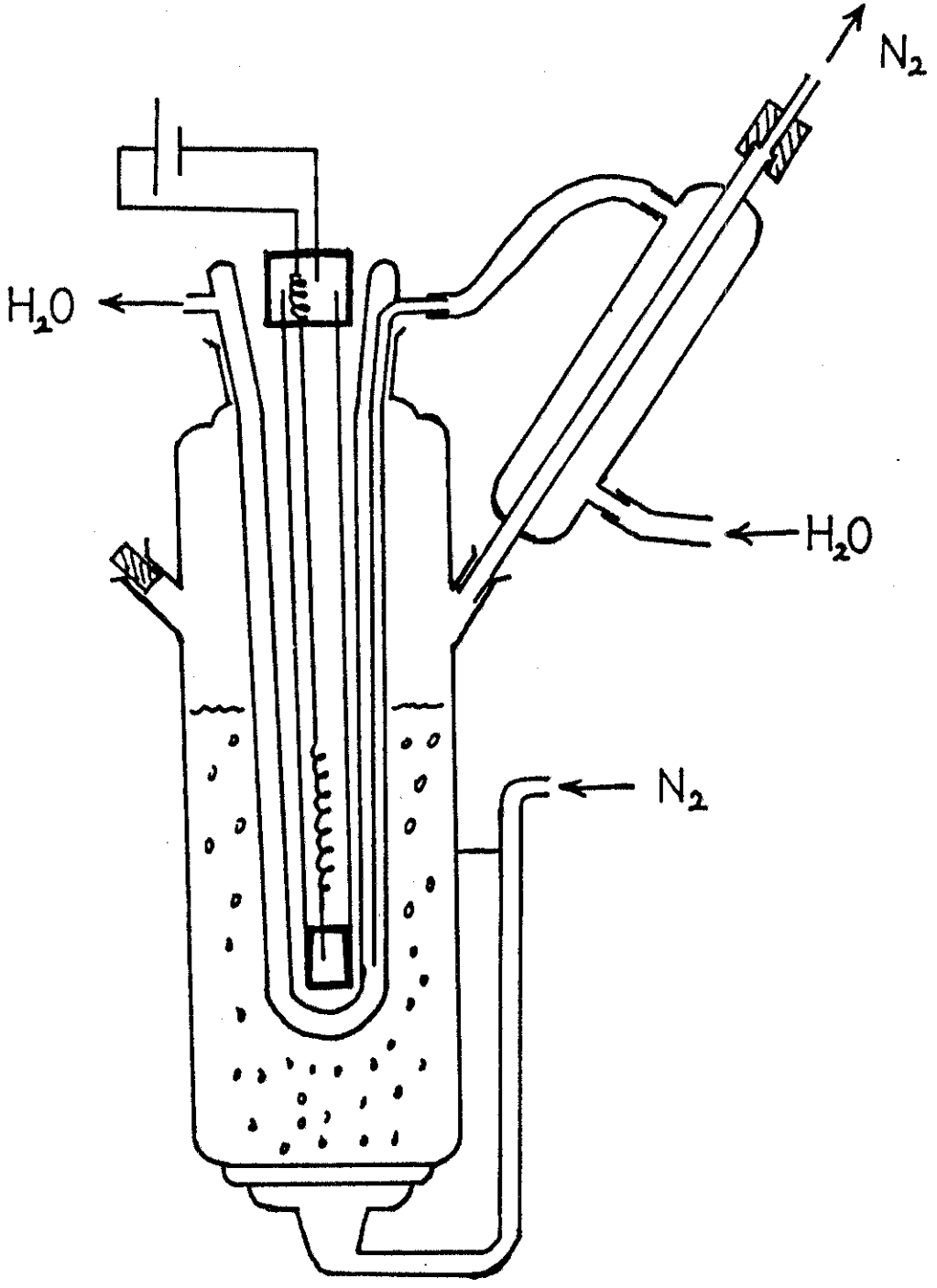


Figure 8. The apparatus for synthesizing the $(DTN)W_2(CO)_{10}$ complex.

values. One and 1.5 g of purified DTN were added and the reaction mixture was photolysed again for 0.5 h. Most of the THF was removed from the reaction mixture under vacuum at 30 $^{o}C$, and the residue was cooled in the freezer for 8 h. The yellow product precipitated from the solution and was collected by filtration and recrystallized from a toluene/ hexane solution (5:1 ratio). The yield of this reaction is 73 % (5.28 g).

The carbonyl stretching frequencies of $(DTN)W_2(CO)_{10}$ in $C_2H_4Cl_2$ exhibited bands 2070 $cm^{-1}$(s) and 1940 $cm^{-1}$(vs) which indicated the presence of the $W(CO)_5$ moiety as shown in Figure 9, confirming Yang's work (1). The NMR spectra of DTN, $(DTN)W(CO)_4$ and $(DTN)W_2(CO)_{10}$ were obtained by Yang as shown in Figure 10, 11 and 12 (1). The methylene group bound to a sulfur atom, which is in turn bound to a tungsten atom, exhibits a slight downfield chemical shift relative to a methylene group attached to a sulfur not bonded to a metal. Comparing the NMR spectra of $(DTN)W(CO)_4$ and $(DTN)W_2(CO)_{10}$ shown in Figure 11 and 12 to that of DTN shown in Figure 10, the triplet peaks of $(DTN)W(CO)_4$ and $(DTN)W_2(CO)_{10}$ showed identical shifts at 3.00 ppm, whereas triplet peaks of DTN occurred at 2.60 ppm. This shifting of the triplet downfield indicates that $(DTN)W_2(CO)_{10}$ was a bridged compound. Anal. Calcd. for $C_{21}H_{24}O_{10}S_2W_2$: C,29.04; H,2.77. Found: C,29.48; H,3.08. These data also indicate that $(DTN)W_2(CO)_{10}$ is a bridged compound (1).

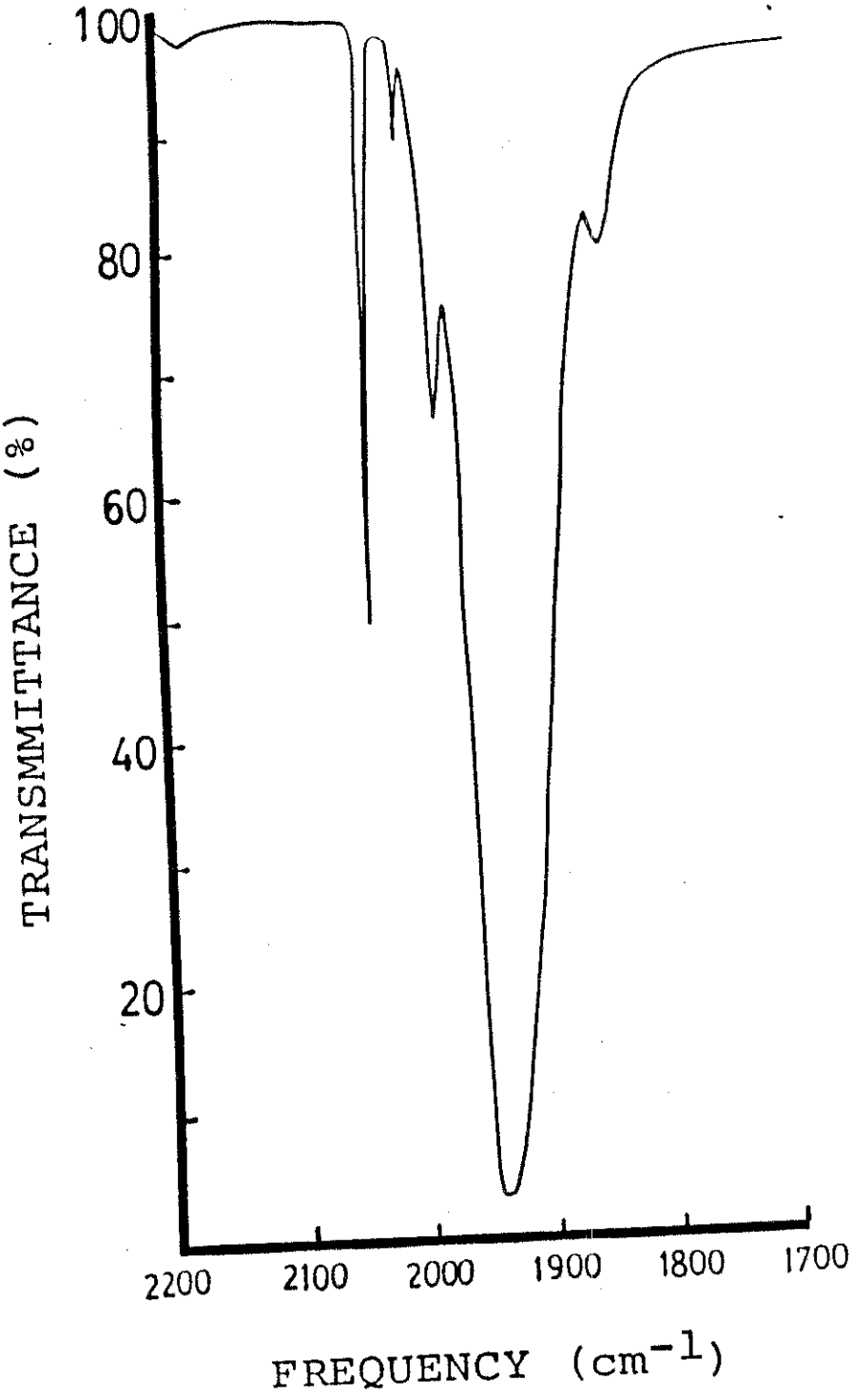


Figure 9. Infrared spectrum of $(DTN)W_2(CO)_{10}$.

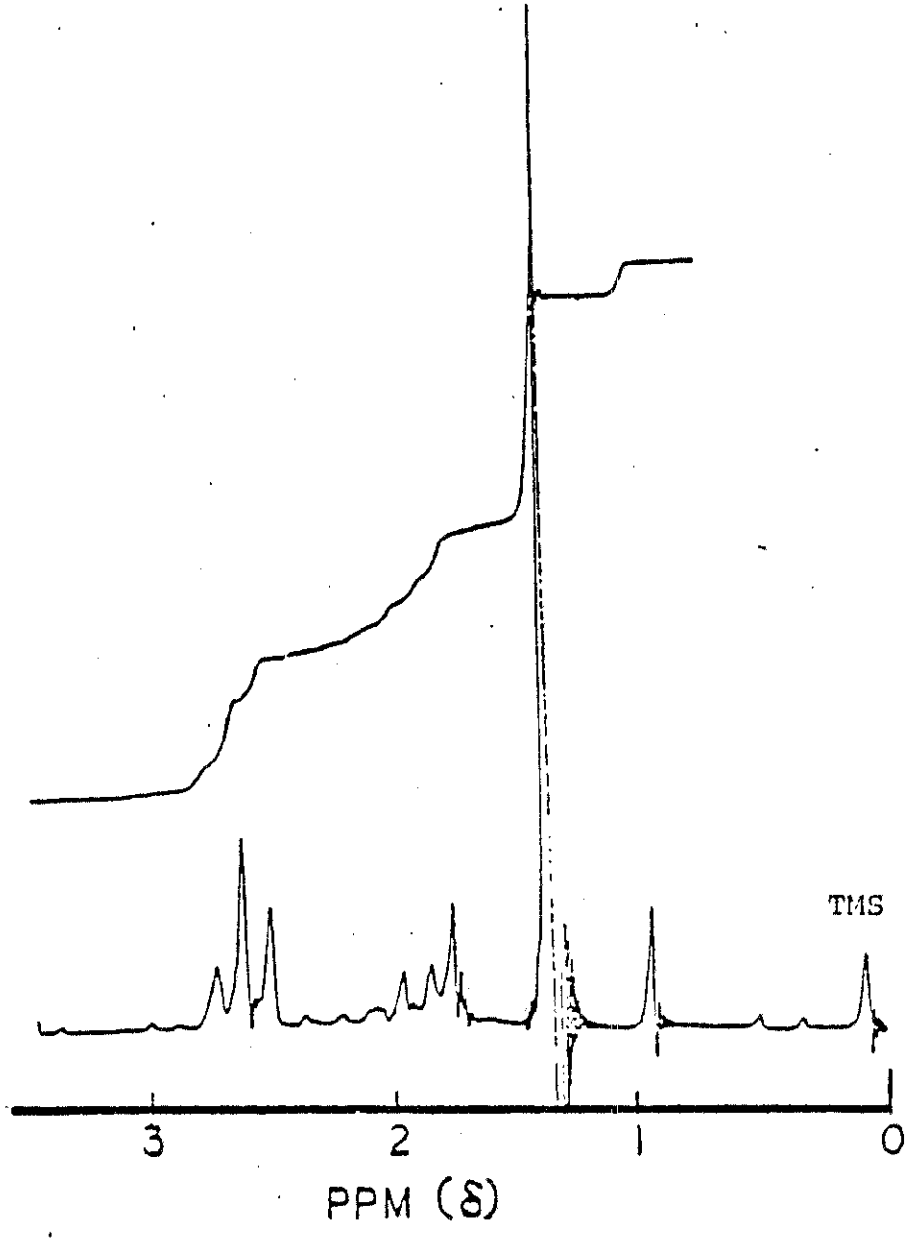


Figure 10. NMR spectrum of DTN. Adapted from S. N. Yang's Thesis, 1982, p. 15.

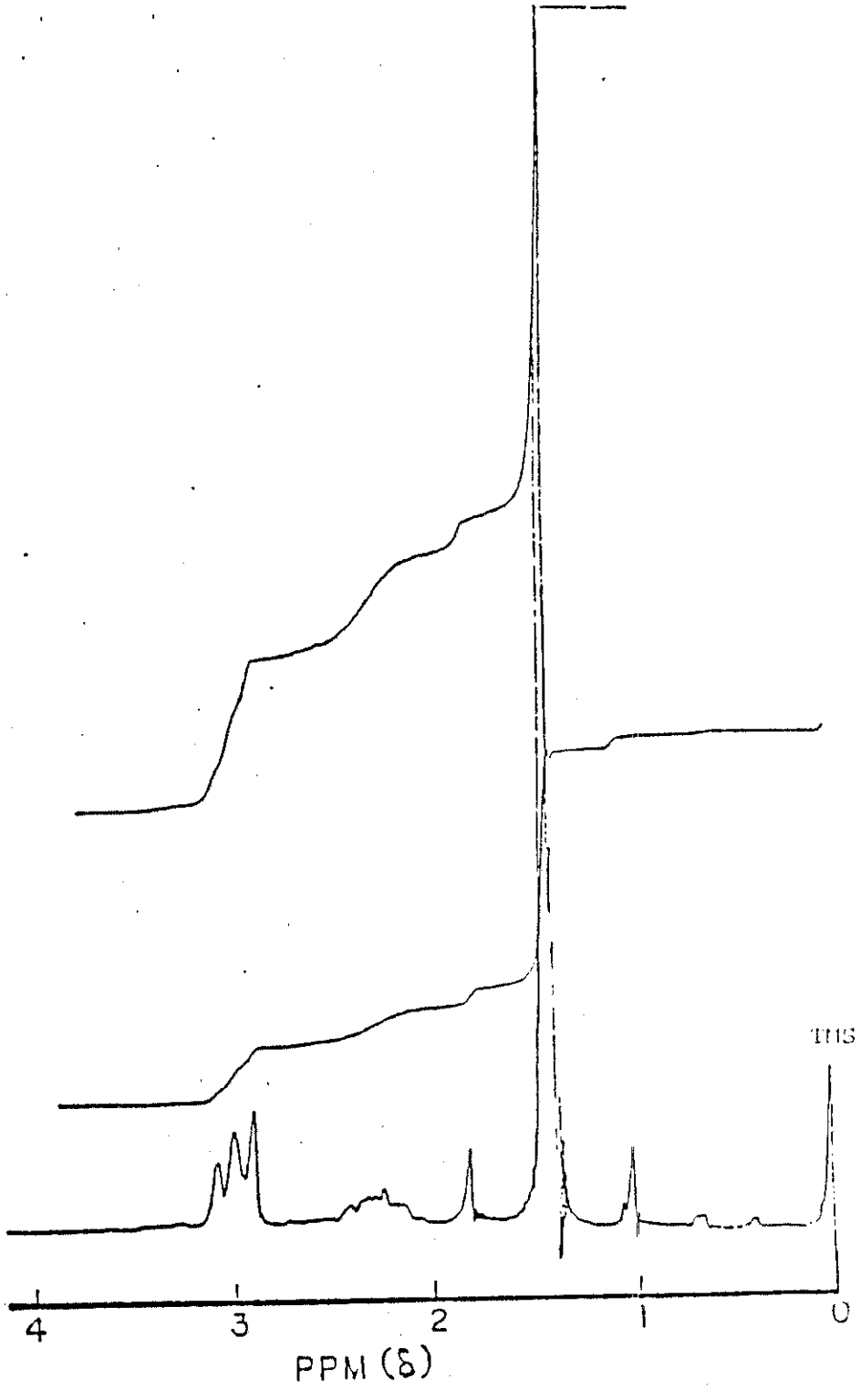


Figure 11. NMR spectrum of $(DTN)W(CO)_4$. Adapted from S. N. Yang's Thesis, 1982, p. 16.

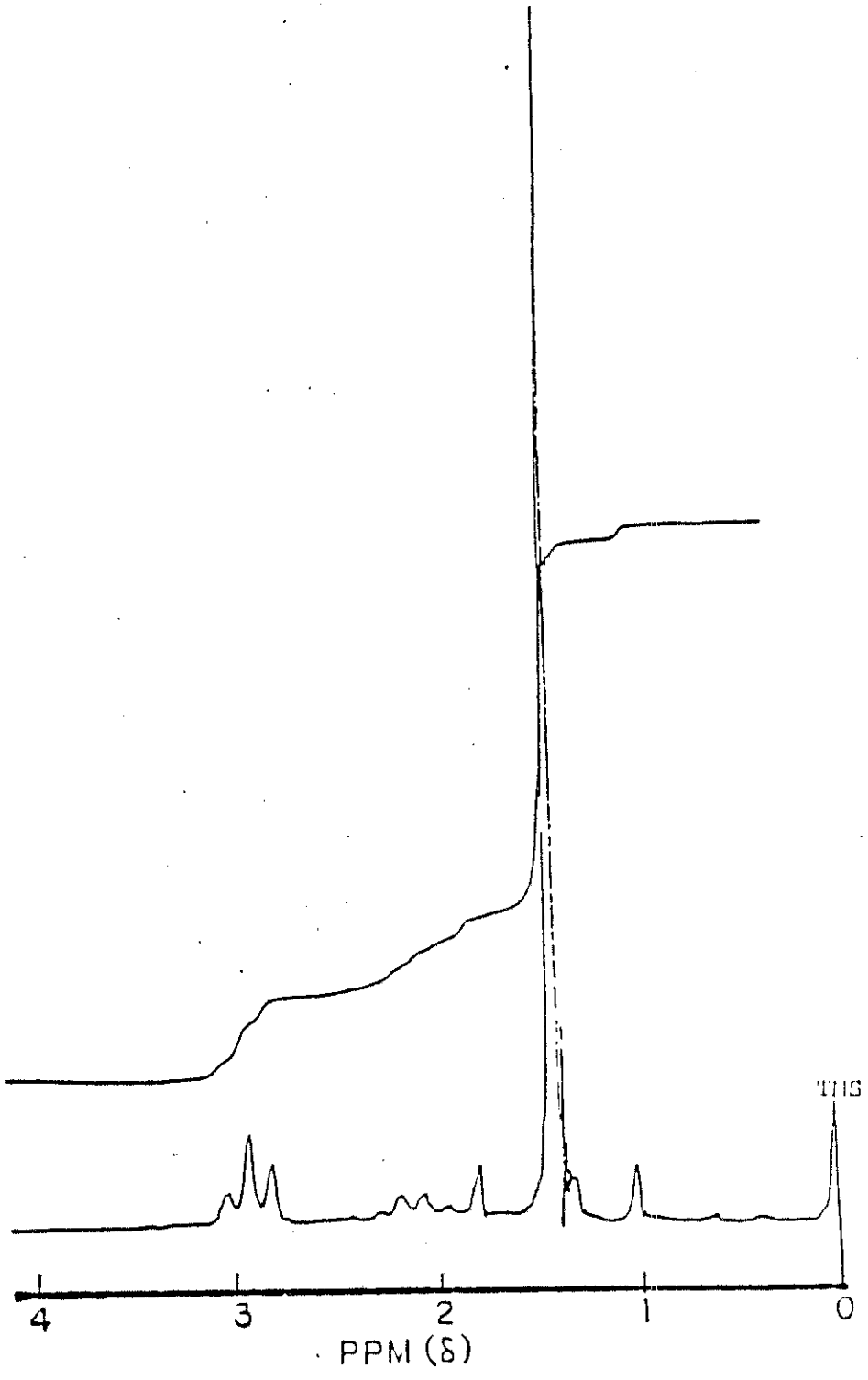


Figure 12. NMR spectrum of $(DTN)W_2(CO)_{10}$. Adapted from S. N. Yang's Thesis, 1982, p. 17.

Conditions of the Reactions. The mechanism of the reaction suggested by Yang and the reaction rates determined at 425 nm were reinvestigated to address the following question: Are the products of this reaction not a monosubstituted complex, and, is the absorbance of this product at 425 nm large enough to influence the determination of reaction rates? Wavelength selection and product varification are necessary before rate determination.

A 25 mL volumetric flask containing 0.196 M $P(OCH(CH_3)_2)_3$ and $2.120 \times 10^{-3}$ M $(DTN)W_2(CO)_{10}$ in 1,2-dichloroethane solvent was placed in a 65 $^oC$ water bath and the solution was left to react for at least 2 days, during which its color changed from yellow to colorless. The UV spectrum of this reaction solution were monitored at three different wavelengths (425 nm, 430 nm and 435 nm) using 0.196M $P(OCH(CH_3)_2)_3$ in 1,2-dichloroethane as the blank. Blank values, $A_{bl} = 0.013$, $A_{bl} = 0.008$ and $A_{bl} = 0.005$ were obtained for the respective wavelengths. The wavelength at 435 nm was selected to use in the determination of reaction rates due to the smaller absorbance of the blank.

The IR spectrum of $(DTN)W_2(CO)_{10}$ as shown in Figure 9 is the same as that of $(DTN)W_2(CO)_{10}$ obtained by Yang (1). The product of this reaction solution was identified by monitoring the carbonyl stretching frequencies as shown in Figure 13, which was similar to those of the $(L)W(CO)_5$ complexes, which were compared and characterized independently (2). Therefore,

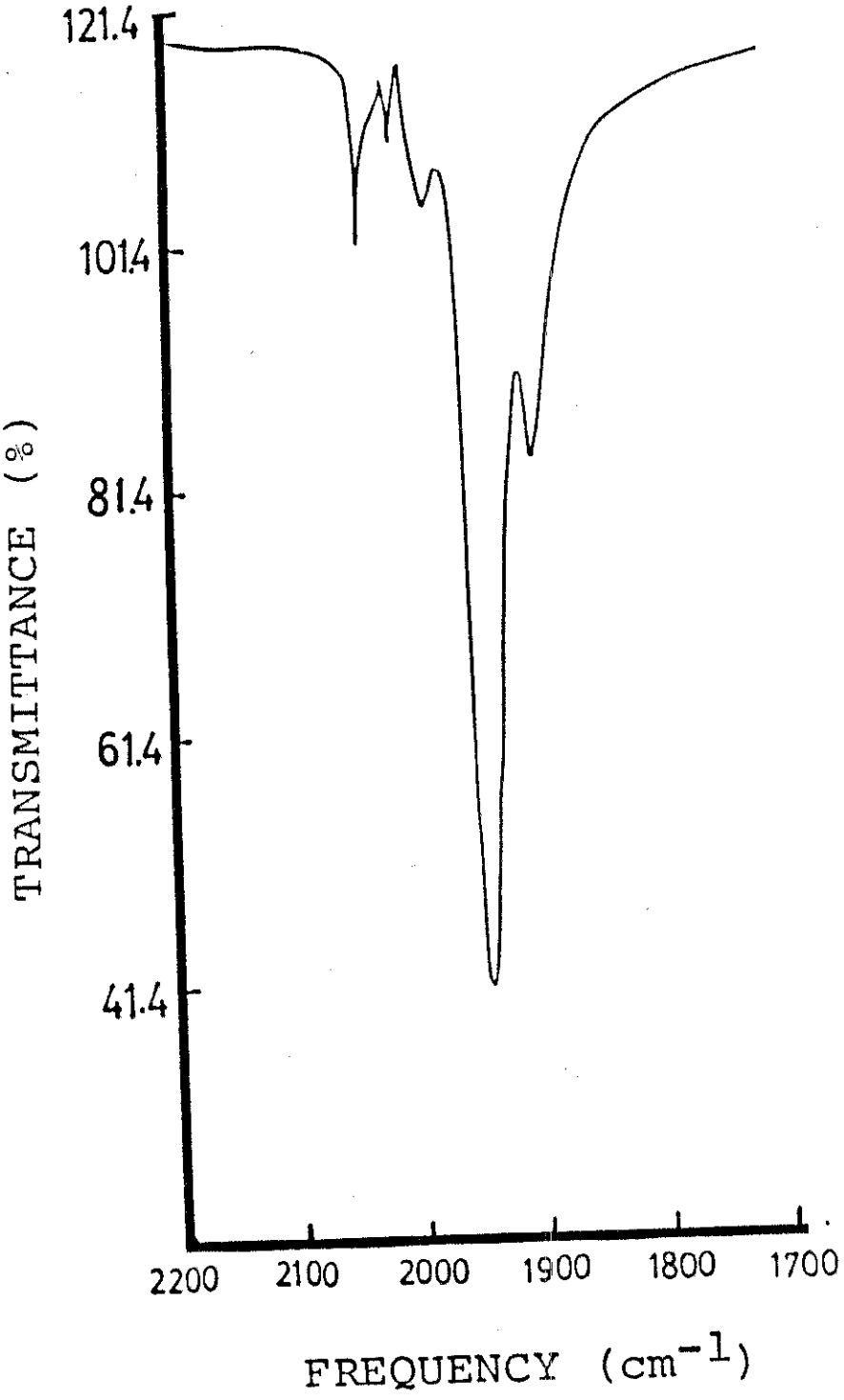


Figure 13. Infrared spectrum of the products of reaction of $(DTN)W_2(CO)_{10}$ with $P(OCH(CH_3)_2)_3$ in 1,2-dichloroethane.

the C-O stretching frequencies of the product of this reaction solution at 2073.6 $cm^{-1}$, 1942.0 $cm^{-1}$ and 1903.8 $cm^{-1}$ as shown in Figure 13 indicate that this product is the monosubstituted complex $P(OCH(CH_3)_2)_3W(CO)_5$.

Rate Determination. The reaction rates were determined by measuring the absorbance of substrate on a Beckman DU-2 spectrophotometer.

Method A. For each kinetics run, a 100 mL volumetric flask was equipped with a stopcock and a rubber septum to prevent contamination of the reaction solution from air and the septum. The flask was then charged with $1.5 \times 10^{-4}$ moles of substrate. A second flask (50 mL) was charged with a weighed amount of triisopropyl phosphite, and was filled to about 40 ml with 1,2-dichloroethane. Both flasks were placed in a thermal water bath which was connected to a Haake Model R21 constant temperature circulator under a fixed constant temperature. The temperature was allowed to equilibrate and the solvent-ligand flask was then filled to 50 mL with solvent. This solution was added into the 100 mL substrate flask. The flask was purged with nitrogen and shaken to ensure complete dissolution of the substrate. Ten minutes were allowed for thermal equilibrium to be reached before the first sample was withdrawn by use of a glass syringe equipped with a ten inch syringe needle. Three mL of nitrogen were injected into the reaction vessel before each sample was withdrawn at different time intervals. Each sample was

analyzed immediately using a 1 cm pyrex cell at 435 nm. The above procedures followed Yang's method (1).

Method B. For each kinetics run, a 10 mL volumetric flask was charged with 0.0265 g of substrate. Another 25 mL volumetric flask was charged with 0.2603 g to 4.6854 g of triisopropyl phosphite, and was filled with about 20 mL of 1,2- dichloroethane. Both flasks were placed in a constant temperature water bath equipped with a Haake Model R21 constant temperature circulator. After the solution reached thermal equilibrium, the solvent-ligand flask was then filled to 25 mL with solvent. The 10 mL substrate flask was filled with this ligand solution. The remaining ligand solution was used as a blank, whose absorbance was determined before the absorbance of the solvent-ligand-substrate solution was monitored. After being shaken and placed in the water bath for 5 minutes, the solvent-ligand-substrate solution was poured into a 1 cm pyrex cell sealed with a rubber-septum. Then, the cell was immediately placed in the water bath. Each sample was analyzed immediately, and was then quickly placed in the water bath for the next determination. After a predetermined time passed, the sample was analyzed again. This was repeated for at least two half-lives of time passed. Whether Method A or Method B is used, each kinetics run must be carried out over at least two half-lives. The absorbance range was about 1.15 to 0.25 absorbance units. One result is shown in Figure 14. From the plot, it can be seen that the

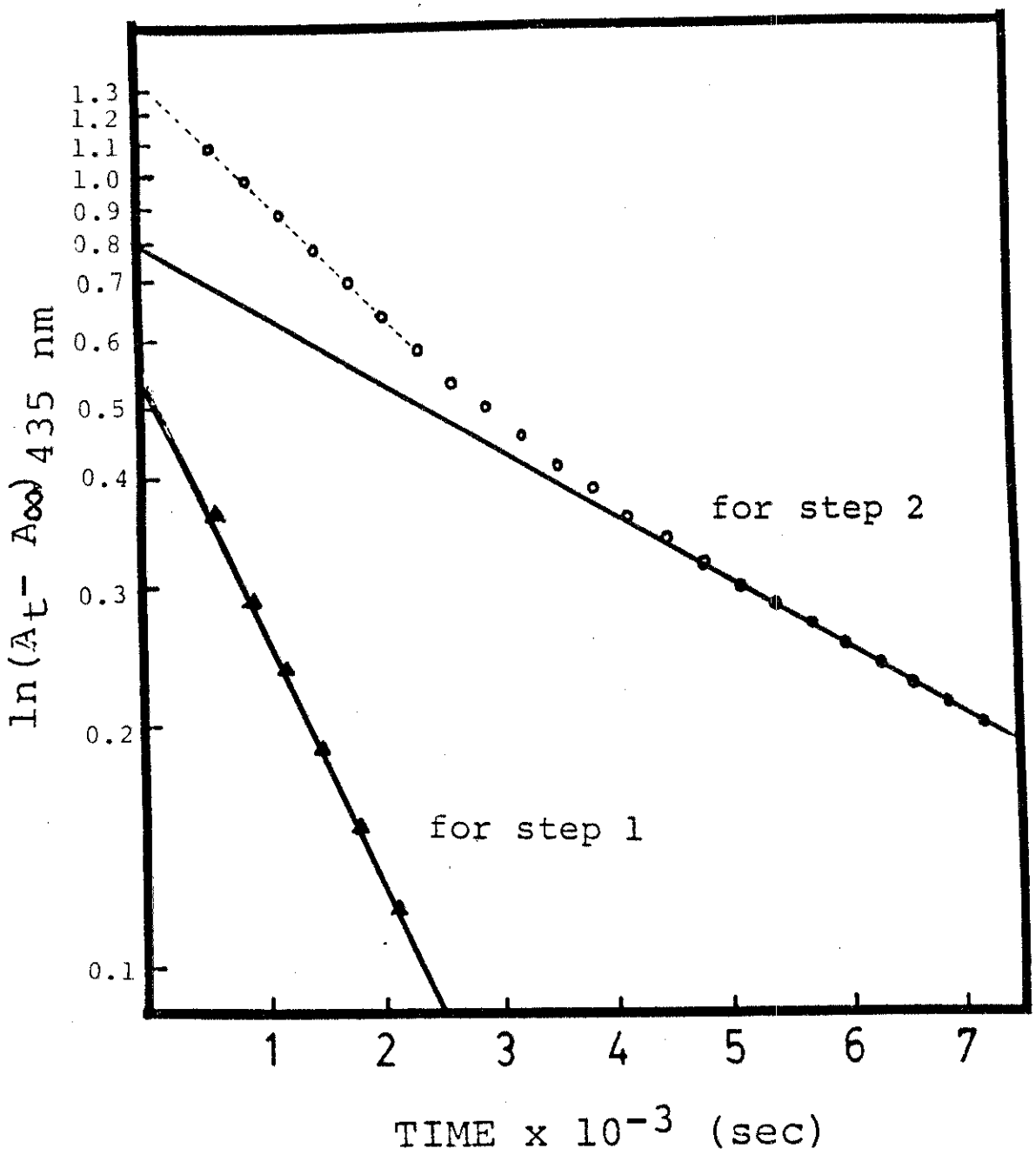


Figure 14. Plot of $\ln A_{correct}$ vs. time for reaction of $(DTN)W_2(CO)_{10}$ with triisopropyl phosphite in 1,2-dichloroethane at 333 °K. (Dash line indicates the first segment, solid line beginning at t = 4500 sec indicates the second segment, and ▲ indicates the corrected data for step 1.)

reaction is stepwise, first order reaction. The absorbance value at $t = \infty$, $A_\infty$, could be measured by determining the absorbance value of the reaction sample after ten half-lives. The solvent-ligand blank $A_{bl}$ instead of $A_\infty$ was used in the plot of $\ln(A_t - A_\infty)$ versus time because the value of $A_\infty$ was nearly equal to that of $A_{bl}$.

In order to ensure an accurate calculation of the rate constants, the sampling was chosen in such a way as to have samplings above A = 0.50 for step 1 and below A = 0.37 for step 2. Based on the principles of consecutive reactions and reaction intermediates shown in Espenson (3), the equations

$$A_t - A_\infty = ß(\exp)(-k'_{obsd}t) + \partial(\exp)(-k_{obsd}t) \text{ ----- (2-1)}$$

$$\Delta = A_t - A_\infty - ß(\exp)(-k'_{obsd}t) = \partial(\exp)(-k_{obsd}t) \text{ -- (2-2)}$$

here, $ß = \text{anti } \ln(r)$

$$\ln \Delta = \ln \partial - k_{obsd}t \text{ ---------- (2-3)}$$

are followed. When $k_{obsd} >> k'_{obsd}$, equation 2-1 can reduce to

$$A_t - A_\infty \approx ß(\exp)(-k'_{obsd}t) \text{ ---------- (2-4)}.$$

From the values of slope, $-k'_{obsd}$, and intercept, r, in the plot of $\ln (A_t - A_\infty)$ vs. time for step 2 as shown in Figure 14, $k'_{obsd}$ and ß can be obtained. The values of $\Delta$ for step 1 can

be also calculated. From the plot of ln $\Delta$ vs. time for step 1 as shown in Figure 14, the value of $k_{obsd}$ can be obtained.

Influence of Excess DTN in the Substitution Reaction. In order to determine whether excess DTN will influence the reaction of $(DTN)W_2(CO)_{10}$ with $P(OCH(CH_3)_2)_3$ in 1,2-dichloroethane, DTN, in a quantity equal to $(DTN)W_2(CO)_{10}$ ($3,1 \times 10^{-3}$ M) was added to a 0.6 M $P(OCH(CH_3)_2)_3$ solution in 1.2-dichloroethane at 60.0 °C. The reaction was also carried out under the same conditions but without DTN.

Changes in the IR Spectra over the Reaction's Course. Using 0.9 M $P(OCH(CH_3)_2)_3$ in 1.2-dichloroethane at 60.0 °C as a blank, a $3.1 \times 10^{-3}$ M solution of $(DTN)W_2(CO)_{10}$ was allowed to react with 0.9 M $P(OCH(CH_3)_2)_3$ in 1,2- dicholorethane solvent, employing Method A. The IR spectrum of this reaction was obtained at intervals of 10 min over two half-lives. The reaction was allowed to proceed until the color of this solution had changed from yellow to colorless, and the IR spectrum of this solution was again obtained.

## Experiment II

Instruments for Flash Photolysis Reactions. Spectroscopic detection of transients produced by the xenon lamp excitation by means of a xenon-discharged capacitor controlled by a pulse sequence generator built in-house was developed in G. R. Dobson's lab. The components of this system and its interconnections are shown in Figure 15 which is similar to that system developed at CFKR (4). The monitoring source was

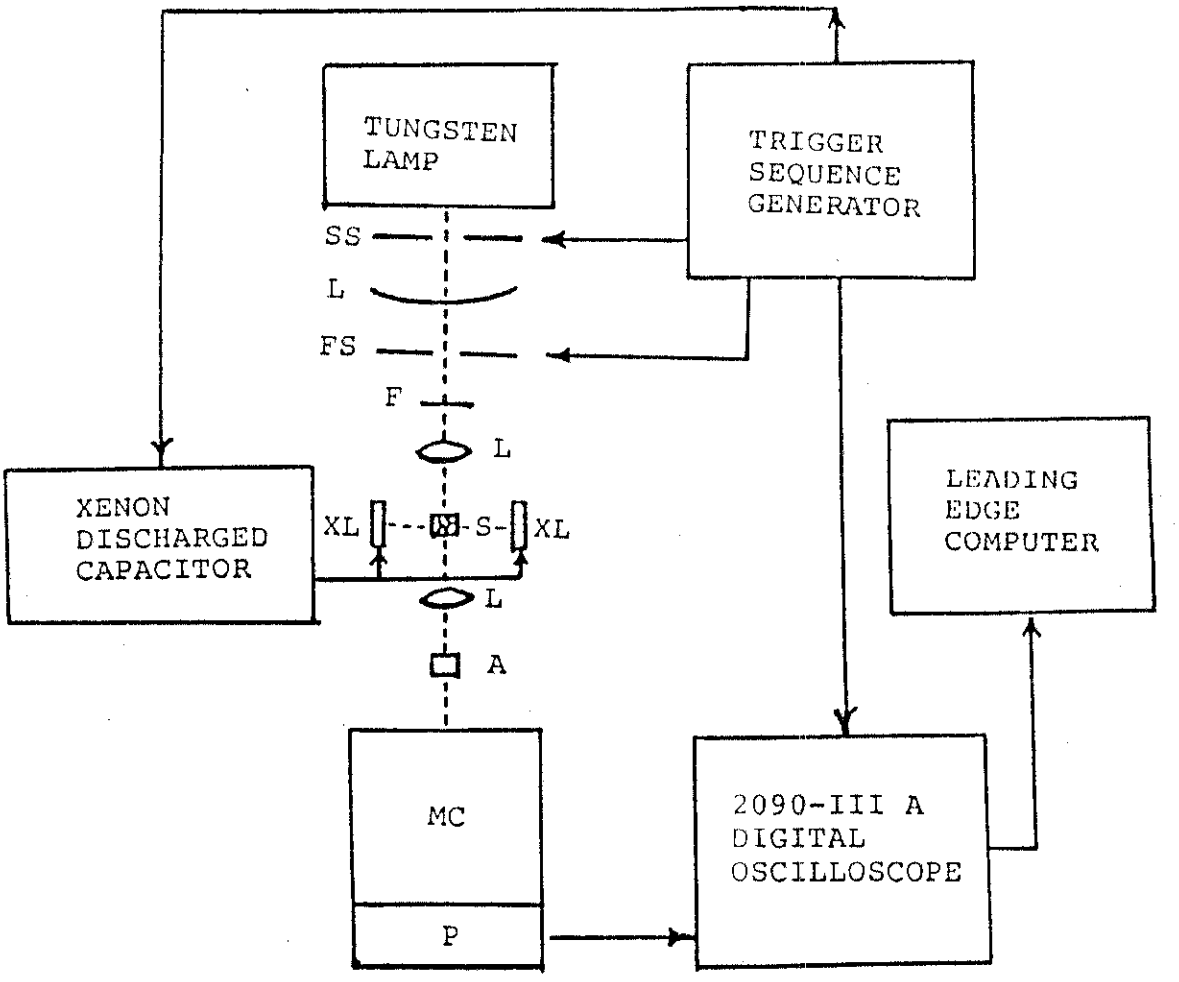


Figure 15. Schematic of Xenon flash photolysis equipment: SS, slow shutter; FS, programmable fast shutter; F, filter; L, lens; S, sample; A, attenuator; MC, monochromator; P, photomultiplier tube; XL, Xenon lamp.

a 40W tungsten lamp placed at right angles to the incident xenon light beam. In order to protect the sample and the detector from continuous irradiation by the analyzing source, two shutters were placed in the analyzing path. The slow shutter remained open for about one second, while the programmable fast shutter open time was variable up to about 10 msec. When a xenon analyzing source is used, the slow shutter is used to avoid burning of the fast shutter due to the analyzing light beam. The exciting and analyzing beams were focussed on openings in the sample holder such that the two beams intersected within the first two or three millimeters of the sample on the exciting side. The opening for the analyzing beam was smaller than that for exciting beam so that the monitoring light would contact only the portion of the sample with the highest concentration of excited species.

The transmitted analyzing light was focussed onto the entrance slit of a Bausch and Lomb monochromator and was detected by a photomultiplier tube (Hamamatsu IP 28) placed at the exit slit. Since the transient signal is often quite small relative to the voltage due to the initial light level $I_o$, the latter was offset and measured by means of an electronic backoff so that the subsequent changes in voltage, $\Delta I$ ($= I_o - I_t$), due to the chemical or physical process in the sample, could be precisely measured. The outputs of both the photomultiplier tube and the back-off were digitized by means of a Nicolet 2090-IIIA digital oscilloscope. The output

waveforms were then read into a Leading Edge computer for kinetic analysis and storage.

Each kinetics run was initiated by a pulse from the computer to the trigger sequence generator, which in turn produced pulses to discharge a high voltage capacitor and thus fired the xenon lamps, opened shutters in the monitoring light path, and triggered the oscilloscope to accept the data.

Rate Determination via Flash Photolysis. For each kinetics run, a 25 mL volumetric flask was charged with a measured amount of triisopropyl phosphite, and filled to about 20 mL with 1,2-dichloroethane. This flask was placed in a Haake Model R21 constant ciculator under a fixed constant temperature (31.1 $^{o}$C). The temperaure was allowed to equilibrate and the solvent-ligand flask was then filled to 25 mL with the solvent. 12.50 mg of $W(CO)_6$ complex was then added into the solvent-ligand flask. After having been shaken for three minutes to ensure complete dissolution of the complex $W(CO)_6$, this solution was poured into a thermal-equilibrium flash cell which was connected to a Haake Model R21 constant temperature circulator under a fixed constant temperature. Each sample was analyzed at 430 nm.

## Chapter Bibliography

1. Yang, S. N. Masters Thesis, North Texas State University, 1982.

2. Angelici, R. J.; Malone, M. D. Inorg. Chem. 1967, 6, 1731.

3. Espenson, J. H. Chemical Kinetics and Reaction Mechanism, McGraw Hill: New York; 1981, 22-24.

4. Linding, B. A.; Rodgers, M. A. J. J. Phys. Chem. 1979, 83, 1683.

# CHAPTER III

## RESULTS

Thermal Reactions. A typical plot $\ln(A_t - A_\infty)$ vs. time for the reaction of $(DTN)W_2(CO)_{10}$ with triisopropyl phosphite is shown in Figure 14. The value of lnA decreased rapidly and linearly from time 0 to time 3000 secs, then decreased slowly but remain linear from time 4500 to time 7000 secs. These results demonstrate that the reaction of $(DTN)W_2(CO)_{10}$ with triisopropyl phosphite is stepwise, first order reaction.

The reaction of $(DTN)W_2(CO)_{10}$ with triisopropyl phosphite in 1,2-dichloroethane was carried out at three temperatures (30.0 $^oC$, 44.5 $^oC$ and 60.0 $^oC$) and various ligand concentrations (from 0.025 M to 0.900 M). Values of $k_{obsd}$ and $k'_{obsd}$ for step 1 and step 2 of the reaction are listed in Table I. The kinetics data showed that both increasing temperature and increasing ligand concentration resulted in increasing the $k_{obsd}$ and $k'_{obsd}$ values of both step 1 and step 2. Figure 16 and 17 graphically summarize Table I; the plots of $k_{obsd}$ for step 1 at 30.0 $^oC$ and 44.5 $^oC$ are not shown because of the scattered data. Reasons for this scattering will be discussed later in this text.

The kinetic results indicate that the rates of the reaction are dependent on both substrate and ligand concentration. The plots of $k_{obsd}$ and $k'_{obsd}$ values for both step 1 and step 2

Table I. Rates of Reaction of (DTN)$W_2(CO)_{10}$ with Triisopropyl Phosphite in 1,2-Dichloroethane

| Temperature °K | Ligand Conc. moles/liter | $k_{obsd}$(step 1) x $10^1$ $sec^{-1}$ | $k'_{obsd}$(step 2) x $10^2$ $sec^{-1}$ |
|---|---|---|---|
| 303.0 | 0.0766 | 0.68(0)* | 1.27(0) |
| | 0.1004 | 1.19(31)* | 1.58(4) |
| | 0.1271 | 0.54(7)* | 1.60(3) |
| | 0.2021 | 0.64(9)* | 1.57(4) |
| | 0.2984 | ------ | 2.15(2) |
| | 0.3997 | 0.89(4)* | 2.33(1) |
| | 0.5009 | 0.89(2)* | 2.42(4) |
| | 0.6006 | 0.99(2)* | 2.47(2) |
| | 0.7005 | 0.72(0) | 2.49(10) |
| | 0.8006 | 1.01(3)* | 2.60(7) |
| | 0.9013 | 1.15(4)* | 2.71(4) |

| Temperature °K | Ligand Conc. moles/liter | $k_{obsd}$(step 1) x $10^0$ $sec^{-1}$ | $k'_{obsd}$(step 2) x $10^1$ $sec^{-1}$ |
|---|---|---|---|
| 317.5 | 0.1019 | 1.17(70)* | 9.50(2) |
| | 0.2021 | 0.26(1) | 1.40(4) |
| | 0.4038 | 0.87(8) | 1.58(5) |
| | 0.6006 | 0.65(4)* | 1.80(1) |
| | 0.8081 | 0.78(5)* | 2.02(10) |

| Temperature °K | Ligand Conc. moles/liter | $k_{obsd}$(step 1) x $10^0 sec^{-1}$ | $k'_{obsd}$(step 2) x $10^1 sec^{-1}$ |
|---|---|---|---|
| 333.0 | 0.0245 | 1.01(2) | 1.22(2) |
| | 0.5051 | 1.11(3) | 2.80(7) |
| | 0.0784 | 1.81(3) | 3.85(10) |
| | 0.1010 | 1.97(4) | 3.74(2) |
| | 0.2011 | 2.03(4) | 5.35(5) |
| | 0.2510 | 2.77(5) | 5.84(7) |
| | 0.2998 | 2.96(8) | 6.12(0) |
| | 0.3503 | 3.02(2) | 6.30(6) |
| | 0.4002 | 3.11(8) | 6.72(6) |
| | 0.4515 | 3.17(5) | 6.84(12) |

Table I. (continued)

| Temperature °K | Ligand Conc. moles/liter | $K_{obsd}$(step 1) x $10^{0}sec^{-1}$ | $k'_{obsd}$(step 2) x $10^{1}sec^{-1}$ |
|---|---|---|---|
| 333.0 | 0.5507 | 3.85(8) | 6.96(12) |
| | 0.6016 | 3.42(7) | 7.14(12) |
| | 0.7000 | 3.28(12) | 6.66(12) |
| | 0.7509 | 3.92(11) | 6.72(6) |
| | 0.8007 | 3.04(5) | 6.72(12) |
| | 0.9027 | 4.12(13) | 7.56(18) |

* indicates that the data are calculated from the initial absorbance of the substrate less than 0.20.

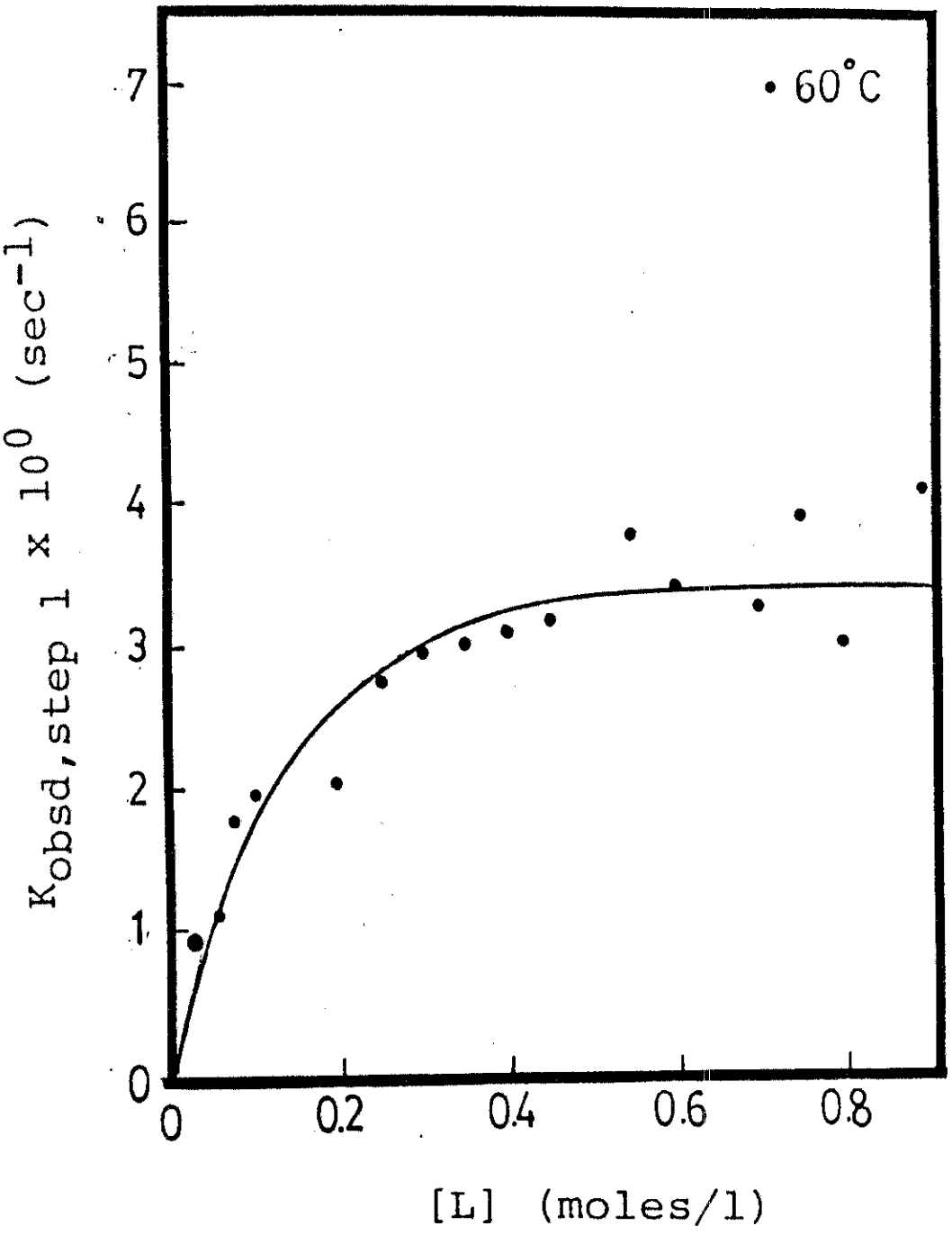


Figure 16. Plot of $k_{obsd}$ vs. [L] for step 1 for reaction of $(DTN)W_2(CO)_{10}$ with triisopropyl phosphite in 1,2-dichloroethane at 333 °K.

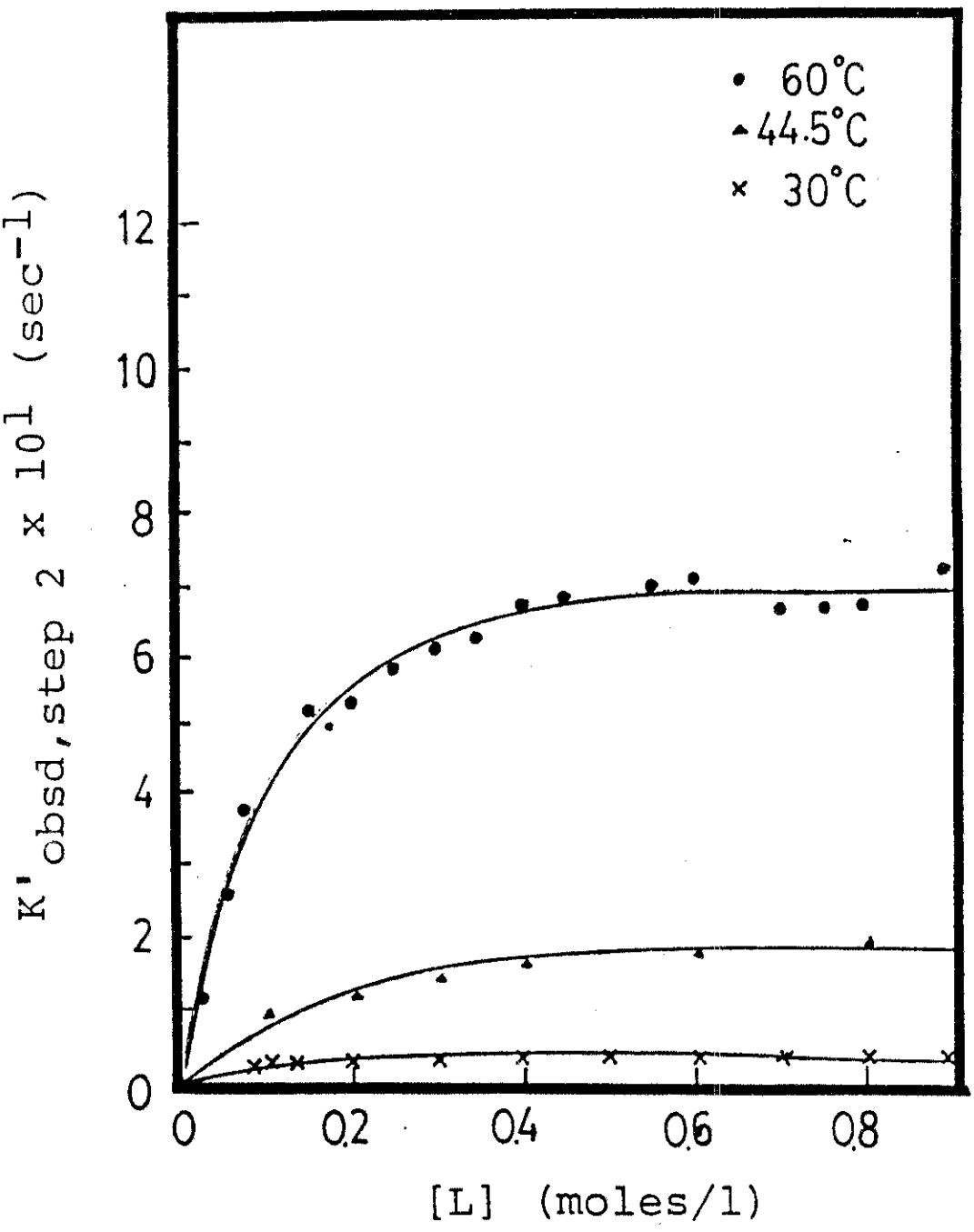


Figure 17. Plot of k'obsd vs. [L] for step 2 for reaction of $(DTN)W_2(CO)_{10}$ with triisopropyl phosphite in 1,2-dicholroethane at different temperatures.

vs. ligand concentration show nonlinear behavior. From the plot of $k_{obsd}$ versus ligand concentration for step 1, a mechanism which is much different from that proposed by Yang will be suggested for step 1. Although plots of $k_{obsd}$ values vs. [L] exhibited nonlinear behavior as shown in Figure 16 and 17, the corresponding reciprocal plots of $1/k_{obsd}$ versus 1/[L] for step 1 and step 2 were linear as shown in Figure 18 and 19 respectively. Comparing the data in Figure 16 and 17 or 18 and 19, one expects that the mechanisms of step 1 and step 2 are similar, and may follow a dissociative and reversible pathway as shown in Figure 20. Following these mechanisms, one can derive the rate laws of step 1 and step 2 as the following equations:

$$-d[(DTN)W_2(CO)_{10}]/dt = \frac{k_{1d}k_2[\text{ligand}]\ [(DTN)W_2(CO)_{10}]}{k_{-1}[(DTN)W(CO)_5] + k_2[\text{ligand}]}$$

for step 1.----------(3-1)

$$-d[(DTN)W(CO)_5]/dt = \frac{k_{3d}k_4[\text{ligand}]\ [(DTN)W(CO)_5]}{k_{-3}[DTN] + k_4[\text{ligand}]}$$

for step 2.----------(3-2)

hence,

$$k_{obsd} = \frac{k_{1d}k_2[\text{ligand}]}{k_{-1}[(DTN)W(CO)_5] + k_2[\text{ligand}]} \text{ ----------(3-3)}$$

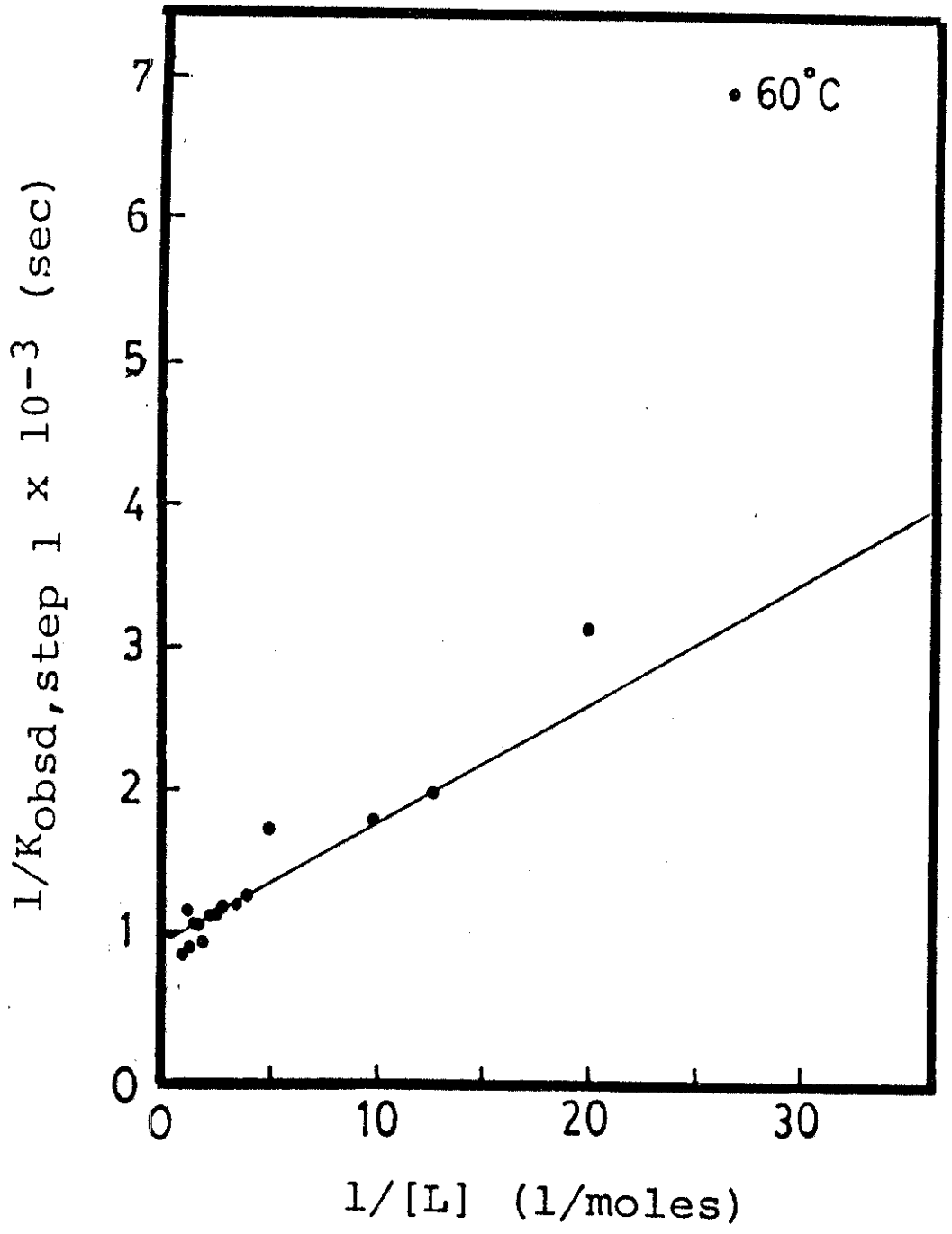


Figure 18. Plot of $1/k_{obsd}$ vs. 1/[L] for step 1 for reaction of $(DTN)W_2(CO)_{10}$ with triisopropyl phosphite in 1,2-dichloroethane at 333 °K.

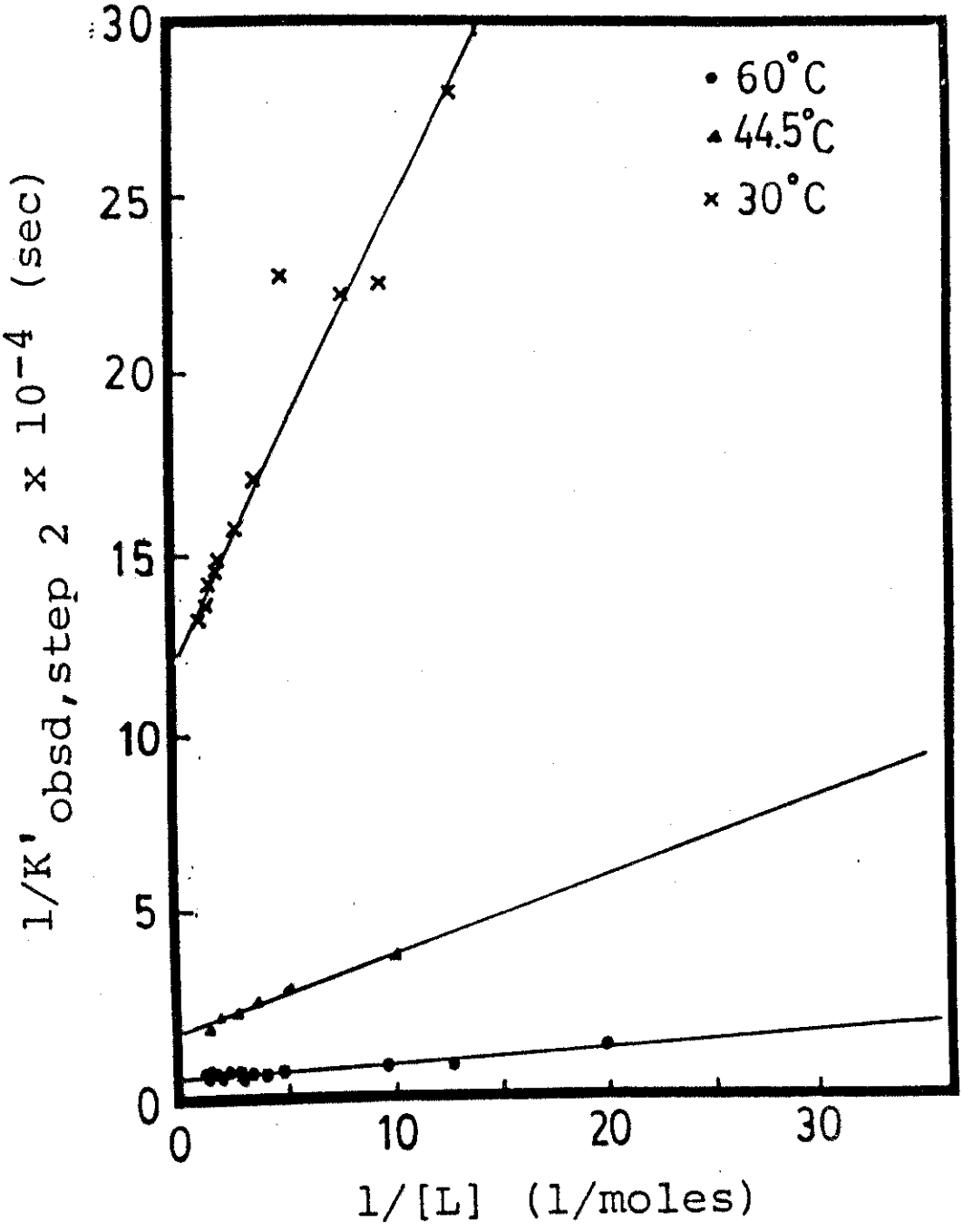


Figure 19. Plot of $1/k'_{obsd}$ vs. 1/[L] for step 2 for reaction of $(DTN)W_2(CO)_{10}$ with triisopropyl phosphite in 1,2-dichloroethane at different temperatures.

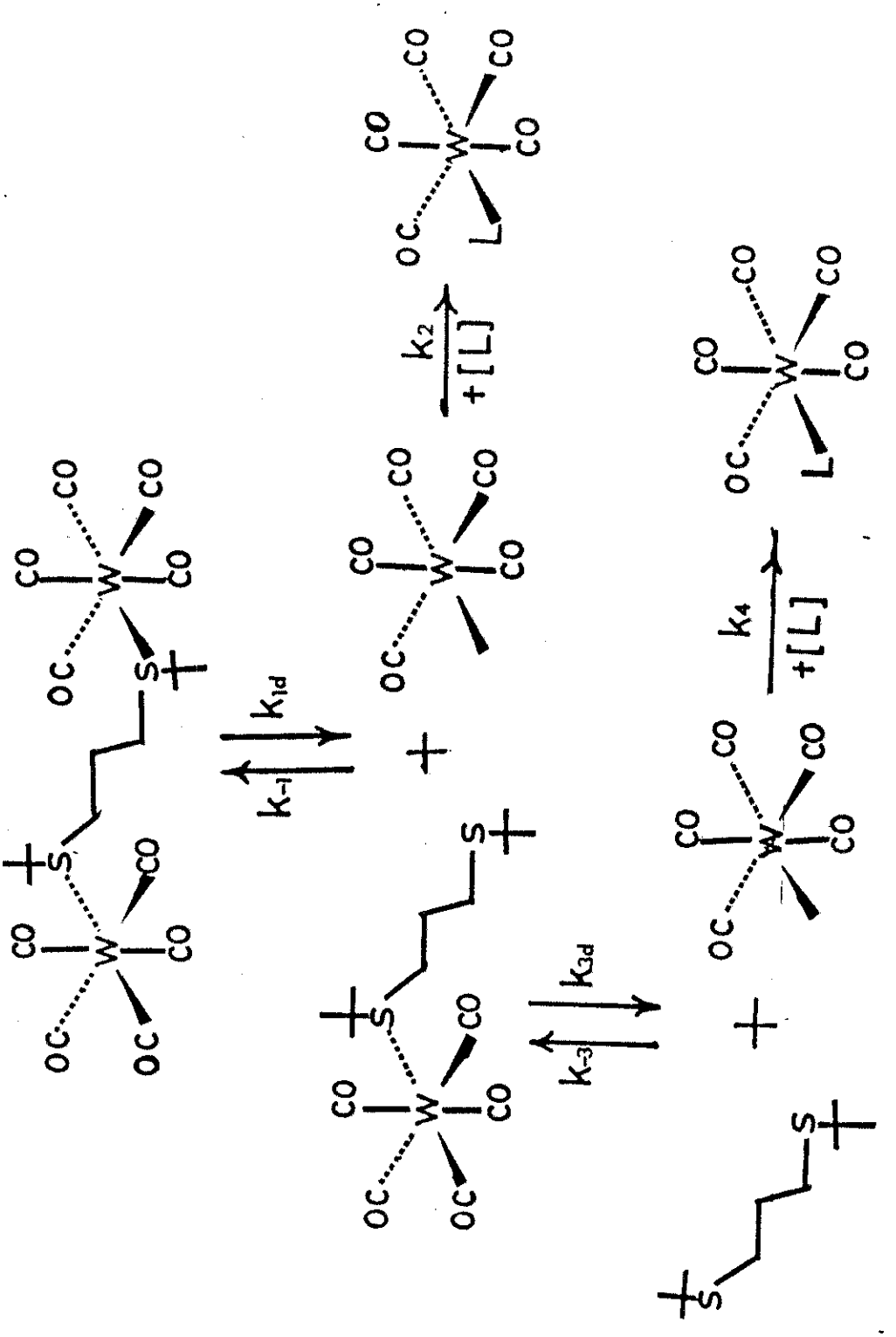


Figure 20. Mechanism I.

$$k'_{obsd} = \frac{k_{3d}k_4[\text{ligand}]}{k_{-3}[\text{DTN}] + k_4[\text{ligand}]} \qquad (3\text{-}4)$$

$$1/k_{obsd} = \frac{k_{-1}[(\text{DTN})W(CO)_5]}{k_{1d}k_2[\text{ligand}]} + \frac{1}{k_{1d}} \qquad (3\text{-}5)$$

$$1/k'_{obsd} = \frac{k_3[\text{DTN}]}{k_{3d}k_4[\text{ligand}]} + \frac{1}{k_{3d}} \qquad (3\text{-}6)$$

Therefore, $k_{1d}$ and $k_{3d}$ can be estimated from the intercept in the plot of $1/k_{obsd}$ versus $1/[L]$. From the above data, we can also calculate the competition rate constants $k_{-1}/k_2$ and $k_{-3}/k_4$. The values of these rate constants and competition ratios at different temperatures are summarized in Table II and III. Here, $k_{1d}$ and $k_{3d}$ are the dissociative rate constants for step 1 and step 2 respectively.

Based on Eyring and Arrhenius equations as shown below,

$$k = \frac{RT}{N_a h} \exp\left(\frac{\Delta S^{\ddagger}}{R}\right) \exp\left(\frac{-\Delta H^{\ddagger}}{RT}\right) \qquad \text{Eyring equation}$$

Avogadro's number is expressed as $N_a$.

$$k = A \exp(-E_a/RT) \qquad \text{Arrhenius equation}$$

two equations can be derived:

Table II. Rate Constants for Reaction of $(DTN)W_2(CO)_{10}$ with Triisopropyl Phosphite in 1,2-Dichloroethane

| Rate Constant | 303.00 °K | 317.50 °K | 333.00 °K |
|---|---|---|---|
| $k_{1d}(sec^{-1})$ | ------ | ------ | $10.28(40) \times 10^{-4}$ |
| $k_{3d}(sec^{-1})$ | $7.99(18) \times 10^{-6}$ | $6.00(30) \times 10^{-5}$ | $2.57(4) \times 10^{-4}$ |

Table III. Competition Ratios for Reaction of $(DTN)W_2(CO)_{10}$ with Triisopropyl Phosphite in 1,2-Dichloroethane

| Competition Ratio | 303.00 °K | 317.50 °K | 333.00 °K |
|---|---|---|---|
| $k_{-1}/k_2$ | ------ | ------ | 21.23(160) |
| $^*k_{-1}/k_2$ | 13.11(12) | ------ | ------ |
| $k_{-3}/k_4$ | 14.95(96) | 21.76(272) | 25.58(48) |

* indicates that the value is calculated from $k^o_{obsd}/k'$ for flash photolysis data in Table V and VI.

$$\frac{d \ln (k/T)}{d (1/T)} = \frac{-\Delta H^{\ddagger}}{R} \qquad \text{----------(3-7)}$$

and

$$\frac{d \ln k}{d (1/T)} = \frac{-E_a}{R} \qquad \text{----------(3-8)}$$

Since the values of $\Delta H^{\ddagger}$ and $\Delta S^{\ddagger}$ are constant over a sufficiently narrow range of temperatures, $\Delta H^{\ddagger}_{individual}$ and $E_a$ can be estimated by using the mean value of individual $\Delta H^{\ddagger}$ and $E_a$ from successive pairs of values of k and T.

$$\Delta H^{\ddagger}_{individual} = \frac{R \ln(k_2 T_1 / k_1 T_2)}{(T_2 - T_1)/(T_1 T_2)} \qquad \text{----------(3-9)}$$

$$E_a = \frac{R \ln(k_2/k_1)}{(T_2 - T_1)/(T_1 T_2)} \qquad \text{----------(3-10)}$$

The value of $\Delta S^{\ddagger}$ is then calculated using the Eyring equation.

Another method for estimating the values of $\Delta S^{\ddagger}$ and $\Delta H^{\ddagger}$ for k is suggested by drawing a plot of ln(k/T) versus 1/T as shown in Figure 21. The linear behavior of this Eyring plot represents the experimental values of rate constant $k_{3d}$ as a function of temperature. The value of $\Delta H^{\ddagger}$ can be estimated from the slope of this plot. The value of $E_a$ can be calculated from the slope in the plot of ln k vs 1/T. From the equation $\Delta G^{\ddagger} = \Delta H^{\ddagger} - T\Delta S^{\ddagger}$, the value of the Gibbs free energy, $\Delta G^{\ddagger}$, can also calculated.

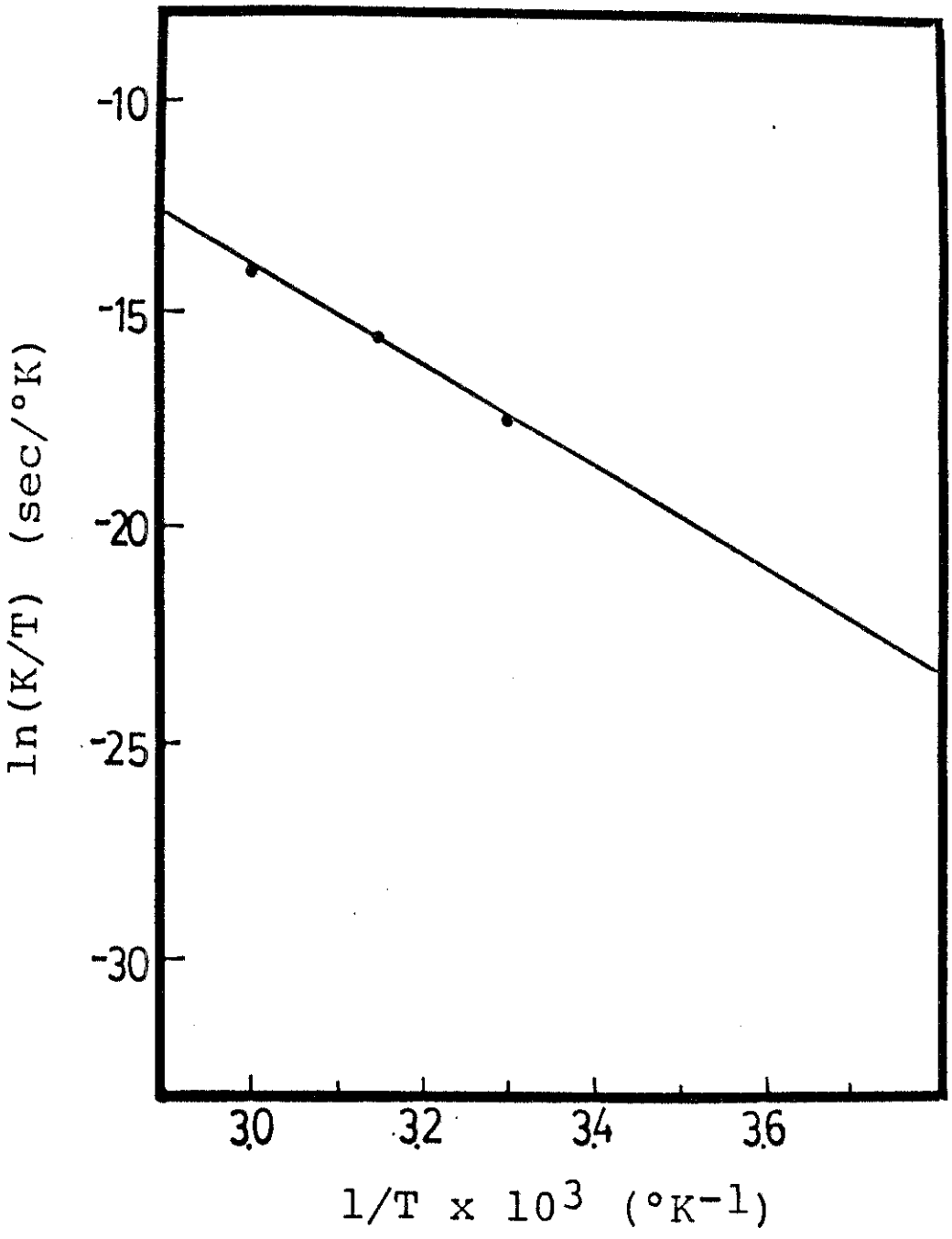


Figure 21. Eyring plot for rate constant $k_{3d}$ of reaction of $(DTN)W_2(CO)_{10}$ with triisopropyl phosphite in 1,2-dichloroethane at different temperatures.

The values of $\Delta H^{\ddagger}$, $\Delta S^{\ddagger}$ and $E_a$ for $k_{3d}$ are listed in Table IV.

Flash Photolysis Reactions. Transient absorbance data stored in the oscilloscope as voltage vs. time can be converted into absorbance vs. time data by using the folowing equation:

$$A_t = \log (I_o/I_t) \quad \text{---------- (3-11)}$$

where $I_o$ is initial light intensity, and $A_t$ and $I_t$ are the optical density and transmitted light intensity at time t.

A typical plot of optical density vs. time for the flash photolysis reaction of $W(CO)_6$ with triisopropyl phosphite in 1,2-dichloroethane is shown in Figure 22. The decay process occurs after the pulse, and the optical density of $W(CO)_5$(solvent) decreases to a constant value after all $W(CO)_5$(solvent) has been converted to $W(CO)_5P(OCH(CH_3)_2)_3$ (1, 2). A plot of $\ln(A_t - A_\infty)$ vs. time is shown in Figure 23. $A_t$ is the optical density at time t, and $A_\infty$ is the optical density of the baseline in Figure 22.

From the slope of the straight line in the plot of $\ln(A_t - A_\infty)$ vs. time as shown in Figure 23, the decay rate constant $k_{obsd}$ of $W(CO)_5$(solvent) can be obtained as shown in Table V. The mechanism of this flash photolysis reaction is expressed as followed:

Table IV. Activation Parameters for Reaction of $(DTN)W_2(CO)_{10}$ with Triisopropyl Phosphite in 1,2-Dichloroethane

| Rate Constant | $E_a$ (Kcal./mole) | $\Delta H^{\ddagger}$ (Kcal./mole) | $\Delta S^{\ddagger}$ (e.u.) |
|---|---|---|---|
| $k_{3d}$ | 23.23(74) | 22.60(141) | -5.73(444) |

Table V. Reaction Rates of the Intermediate Produced by Pulsed Photolysis of $1.42 \times 10^{-3}$ M $W(CO)_6$ under Various Concentrations of Triisopropyl Phosphite at 304.1 $^{o}K$ Monitored at 430 nm

| Ligand Conc. moles/liter | $k_{obsd}$ $\times 10^{-2}$ $sec^{-1}$ | $k'(k_{obsd}/[L])$ $\times 10^{-3}$ $sec^{-1}M^{-1}$ |
|---|---|---|
| 0.1008 | 1.56(0) | 1.43(0) |
| 0.5117 | 6.89(1) | 1.35(2) |
| 0.9993 | 12.64(3) | 1.26(3) |
| | | 1.35(2) (Average) |

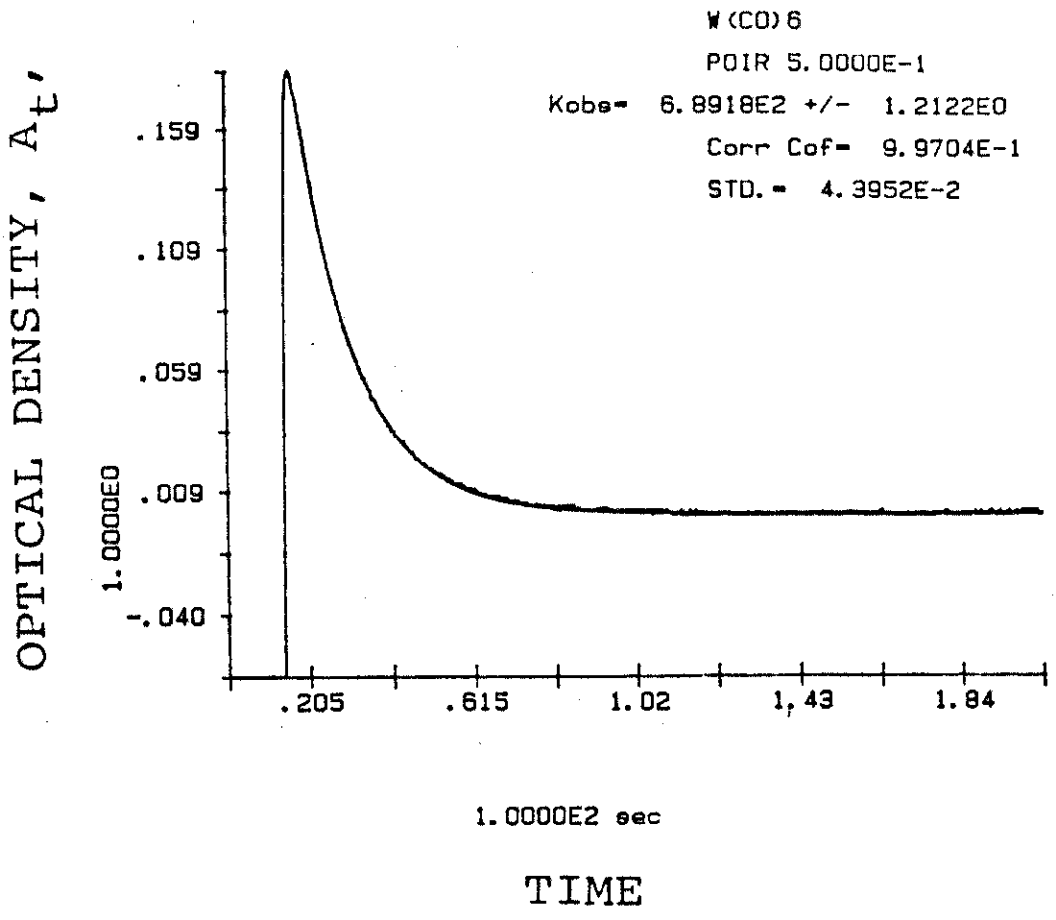


Figure 22. Plot of optical density, $A_t$, vs. time monitored at 430 nm for a 1.42 x $10^{-3}$ M solution of $W(CO)_6$ containing 1.00 M $P(OCH(CH_3)_2)_3$ in 1,2-dichloroethane.

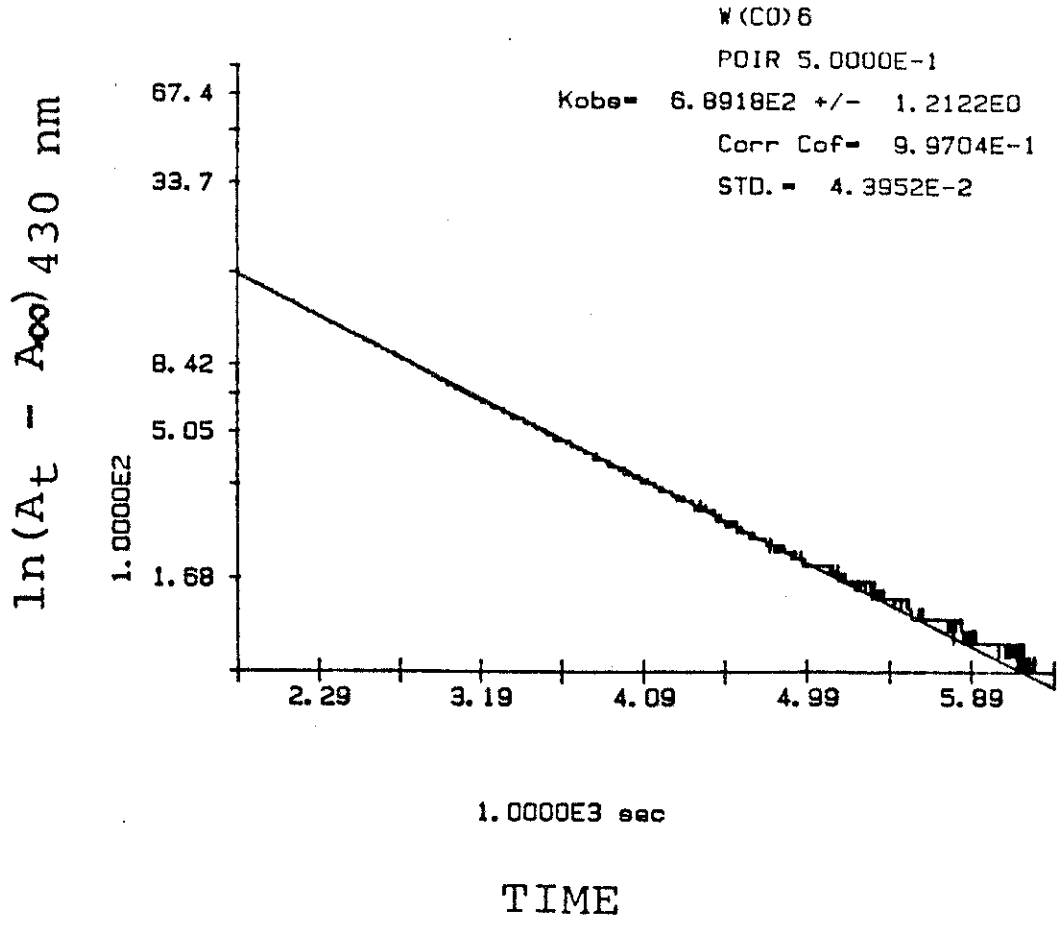


Figure 23. Plot of $\ln(A_t - A_\infty)$ vs. time monitored at 430 nm for a $1.42 \times 10^{-3}$ M solution of $W(CO)_6$ containing 1.00 M $P(OCH(CH_3)_2)_3$ in 1,2-dichloroethane.

$$W(CO)_6 \xrightarrow{h\nu} W(CO)_5 + CO \qquad \text{(3-12)}$$

$$W(CO)_5 + \text{solvent} \underset{k_1}{\overset{k_{-1}}{\rightleftharpoons}} W(CO)_5(\text{solvent}) \qquad \text{(3-13)}$$

$$W(CO)_5 + L \xrightarrow{k_2} W(CO)_5L \qquad \text{(3-14)}$$

therefore, the rate law can be derived

$$\frac{-d[W(CO)_5(\text{solvent})]}{dt} = \frac{k_1k_2[L][W(CO)_5(\text{solvent})]}{k_{-1}[\text{solvent}] + k_2[L]} \qquad \text{(3-15)}$$

since $k_{-1}[\text{solvent}] >> k_2[L]$, the rate law can be simplified to

$$\frac{-d[W(CO)_5(\text{solvent})]}{dt} = \frac{k_1k_2[L][W(CO)_5(\text{solvent})]}{k_{-1}[\text{solvent}]}$$

$$= k'[L][W(CO)_5(\text{solvent})] \qquad \text{(3-16)}$$

where, $k' = (k_1k_2)/(k_{-1}[\text{solvent}])$; therefore , $k_{obsd} = k'[L]$ and k' can be obtained as shown in Table V.

## Chapter Bibliography

1. Dobson, G. R.; Hodges, P. M.; Healy, M. A.; Poliakoff, M.; Turner, J. J.; Firth, S.; Asali, J. J. Am. Chem. Soc. 1987, 109, 4218-4224.

2. Asali, K. J.; Basson, S. S.; Tucker, J. S.; Hester, B. C.; Cortes, J. E.; Awad, H. H.; Dobson, G. R. J. Am. Chem. Soc. 1987, 109, 5386-5392.

# CHAPTER IV

## DISCUSSION

From typical plot $\ln(A_t - A_\infty)$ vs. time for the thermal reaction, it can be seen that the substitution reaction of $(DTN)W_2(CO)_{10}$ with triisopropyl phosphite in 1,2-dichloroethane is stepwise, first order reaction. The plot of $k_{obsd}$ vs. ligand concentration for step 1 is similar to that for step 2 and resembles a hyperbolic curve. There are two alternate mechanisms to explain this reaction pathway.

Mechanism (II) as shown in Figure 24: For step 1, the substrate $(DTN)W_2(CO)_{10}$ is dissociated into the species $W(CO)_5$ and $(DTN)W(CO)_5$. The intermediate $W(CO)_5$ then reacts with $(DTN)W(CO)_5$ to reform $(DTN)W_2(CO)_{10}$ or reacts with triisopropyl phosphite to form the $P(OCH(CH_3)_2)_3W(CO)_5$ product. For step 2, the $(DTN)W(CO)_5$ quickly loses a CO to form $(DTN)W(CO)_4$, a ring closed-complex, then, with subsquent ring opening, forms the $(P(OCH(CH_3)_2)_3)_2W(CO)_4$ product. The rate law derived from the mechanisms for steps 1 and 2 shown in Figure 24 follows the equations:

$$-d[(DTN))W_2(CO)_{10}]/dt = \frac{k_{1d}k_2[\text{ligand}][(DTN)W_2(CO)_{10}]}{k_{-1}[(DTN)W(CO)_5] + k_2[\text{ligand}]}$$

for step 1 ----------(4-1)

$$-d[(DTN)W(CO)_4]/dt = \frac{k_{3d}k_4[ligand][(DTN)W(CO)_4]}{k_{-3} + k_4[ligand]}$$

for step 2 ----------(4-2)

$$\frac{1}{k_{obsd}} = \frac{1}{k_{1d}} + \frac{k_{-1}[(DTN)W(CO)_5]}{k_{1d}k_2} \times \frac{1}{[L]}$$

for step 1 ----------(4-3)

$$\frac{1}{k'_{obsd}} = \frac{1}{k_{3d}} + \frac{k_{-3}}{k_{3d}k_4} \times \frac{1}{[L]}$$

for step 2 ----------(4-4)

Mechanism (I) is shown in Figure 20: Step 1 pathway is the same as that of mechanism (I) in Figure 24. For step 2 pathway, the substrate $(DTN)W(CO)_5$ is dissociated into the species $W(CO)_5$ and DTN. The intermediate $W(CO)_5$ then reacts with triisopropyl phosphite to form $P(OCH(CH_3)_2)_3W(CO)_5$ or with DTN to reform $(DTN)W(CO)_5$. The rate law derived from the mechanisms for steps 1 and 2 shown in Figure 20 follow the equations:

$$-d[(DTN)W_2(CO)_{10}]/dt = \frac{k_{1d}k_2[ligand][(DTN)W_2(CO)_{10}]}{k_{-1}[(DTN)W(CO)_5]+k_1[ligand]}$$

for step 1 ----------(4-1)

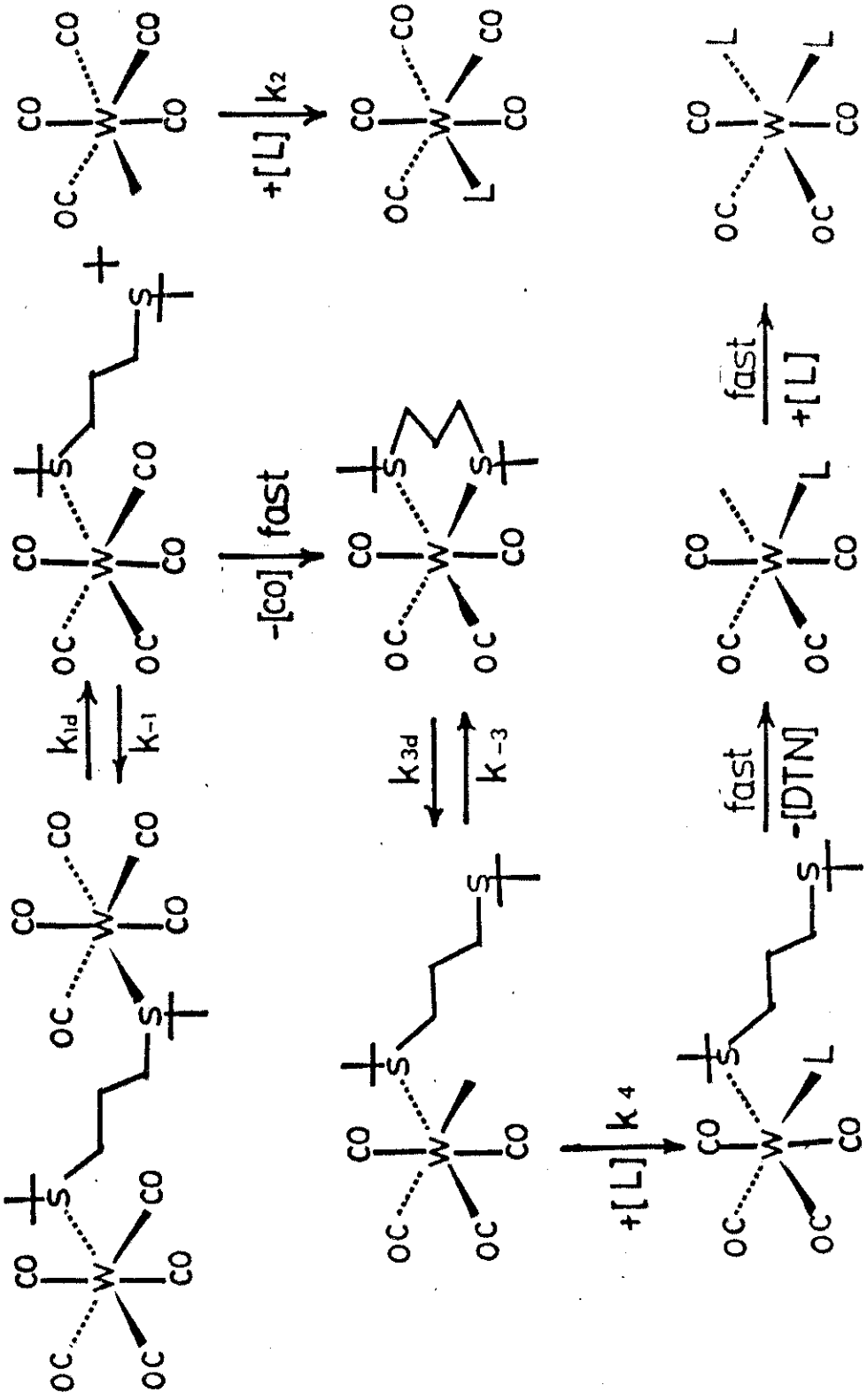


Figure 24. Mechanism II.

$$-d[(DTN)W(CO)_5]/dt = \frac{k_{3d}k_4[ligand][(DTN)W(CO)_5]}{k_{-3}[DTN] + k_4[ligand]}$$

for step 2 ----------(4-5)

$$\text{and} \quad \frac{1}{k_{obsd}} = \frac{1}{k_{1d}} + \frac{k_{-1}[(DTN)W(CO)_5]}{k_{1d}k_2} \times \frac{1}{[L]}$$

for step 1 ----------(4-3)

$$\frac{1}{k'_{obsd}} = \frac{1}{k_{3d}} + \frac{k_{-3}[DTN]}{k_{3d}k_4} \times \frac{1}{[L]}$$

for step 2 ----------(4-6)

From the following data, the mechanisms for steps 1 and 2 shown in Figure 20 and 24 are favored: When $k_2[L] >> k\text{-}1[(DTN)W(CO)_5]$, $k_4[L] >> k_{-3}$, and $k_4[L] >> k_{-3}[DTN]$, the equations (4-1),(4-2) and (4-5) can be simplified to

$$-d[(DTN)W_2(CO)_{10}]/dt = k_{1d}[(DTN)W_2(CO)_{10}] \text{ --------(4-7)}$$

$$-d[(DTN)W(CO)_4]/dt = k_{3d}[(DTN)W(CO)_4] \text{ ----------(4-8)}$$

$$-d[(DTN)W(CO)_5]/dt = k_{3d}[(DTN)W(CO)_5] \text{ ----------(4-9)}.$$

The simplified equation (4-7) is consistent with the data

shown in Figure 16, and the simplified equations (4-8) and (4-9) are consistent with the data shown in Figure 17 in which the values of $k_{obsd}$ and $k'_{obsd}$ will be nearly constant at high concentrations of ligand.

Equation (4-3) is consistent with the data shown in Figure 18, and equations (4-4) and (4-6) are consistent with the data shown in Figure 19 in which plots of $1/k'_{obsd}$ vs. $1/[L]$ and $1/k_{obsd}$ vs. $1/[L]$ are linear.

Although both mechanisms (I) and (II) are supported by the kinetics data as shown in Figure 16, 17, 18 and 19, mechanism (II) as shown in Figure 24 can be ruled out due to the following reasons:

(A) The reaction of $(DTN)W_2(CO)_{10}$ with CO results in the products DTN and $W(CO)_6$; however, $(DTN)W(CO)_4$ does not react with CO under the same reaction conditions (1). Therefore, the possibility of a reaction of $(DTN)W(CO)_5$ in which there is ring closure to afford $(DTN)W(CO)_4$ is eliminated. Mechanism (II) for the step 2 pathway suggested in Figure 24 is not correct since in this mechanism the reaction of $(DTN)W(CO)_5$ proceeds through a step of DTN ring-closure and subsequent displacement of DTN by $P(OCH(CH_3)_2)_3$.

(B) From the IR spectrum of the product of the substitution reaction of $(DTN)W_2(CO)_{10}$ with triisopropyl phosphite in 1,2-dichloroethane, the product, which has carbonyl stretching bands 2076.0 $cm^{-1}$, 1942.2 $cm^{-1}$, and 1900.0 $cm^{-1}$ as shown in Figure 13 has been shown to be a

monosubstituted complex (2, 3 and 4).

Consequently, the rate laws for equations (4-1,5,3 and 6) which are derived from mechanism (I), are as follows:

From the equations (4-3) and (4-6), $1/k_{obsd}$ vs. $1/[L]$ result in linear plots of slope $(1/k_{1d} \times k_{-1}[(DTN)W(CO)_5]/k_2)$ and intercept $(1/k_{1d})$, and slope $(1/k_{3d} \times k_{-3}[DTN]/k_4)$ and intercept $(1/k_{3d})$.

Therefore,

$$\frac{\text{slope}}{\text{intercept}} = \frac{k_{-1}[(DTN)W(CO)_5]}{k_2} \quad \text{for step 1 -------(4-10)}$$

$$\frac{\text{slope}}{\text{intercept}} = \frac{k_{-3}[DTN]}{k_4} \quad \text{for step 2 --------(4-11)}$$

Since the maximum concentration of $(DTN)W(CO)_5$ is about $3.1 \times 10^{-3}$ M and that of DTN is about $6.2 \times 10^{-3}$ M, the value of the competition ratio $k_{-1}/k_2$ at 60.0 °C and those of the competition ratios $k_{-3}/k_4$ at 30.0 °C, 44.5 °C and 60.0 °C as shown in Table III can be calculated. The dissociative rate constants $k_{1d}$ and $k_{3d}$ for step 1 and step 2 at 60.0 °C respectively are also calculated as shown in Table II, and the value of the dissociation rate constant $k_{3d}$ for step 2 is close to that of $k_{2d}$ ($1.7 \times 10^{-4}$ $sec^{-1}$) for step 2 as determined by Yang (1).

It is important to understand whether or not the

concentrations of (DTN)$W(CO)_5$ and DTN will influence the rate constants for step 1 and step 2 of this reaction. Based on the law of mass action, the second segment in the plot of $\ln(A_t - A_\infty)$ vs. time as shown in Figure 14 will be a hyperbolic curve instead of a straight line if the concentration of DTN influences the $k'_{obsd}$ for step 2 of the reaction. In other words, the value of $d \ln(A_t - A_\infty)/dt$ in the second segment under that condition will decrease in proportion to the reaction time. Therefore, it can be predicted that the concentration of DTN will not influence the $k'_{obsd}$ for step 2 in the reaction. From the data shown in Table VII, it can be concluded that the rate constants $k_{obsd}$ and $k'_{obsd}$ are not influenced by addition of the same amount of DTN as substrate (DTN)$W_2(CO)_{10}$ under the same conditions.

The above phenomenon can be explained as follows: It is defined that the effective concentrations of DTN consist of coordinated DTN as (DTN)$W(CO)_5$ and DTN ligand, which both remain in close vicinity to $W(CO)_5$ after dissociation as shown in Figure 25. Although the total concentrations of DTN increase through addition of $3.1 \times 10^{-3}$ M DTN, the effective concentrations of DTN which can influence the reaction are independent of the amount of DTN added and do not change the values of $k_{obsd}$ and $k'_{obsd}$. The same results are obtained as shown in Table VI and in Table VII by adding the same amount of DTN as substrate (DTN)$W_2(CO)_{10}$ under the same conditions.

The values of competition ratios listed in Table III are

Table VI. Reaction Rates of the Intermediate Produced by Pulsed Photolysis of $5.13 \times 10^{-4}$ M $(DTN)W_2(CO)_{10}$ under Different Conditions in 1,2-Dichloroethane at 304.1 $^{o}K$ Monitored at 470 nm

| Triisopropyl Phosphite moles/liter | DTN Added moles/liter | $k_{obsd} \times 10^{-4}$ $sec^{-1}$ |
|---|---|---|
| ------ | ------ | 1.66(4) |
| ------ | ------ | 1.77(10) |
| ------ | ------ | 1.77(13) |
| ------ | $5.13 \times 10^{-4}$ | 1.67(16) |
| $5.10 \times 10^{-4}$ | ------ | 2.20(12) |
| $5.15 \times 10^{-4}$ | ------ | 1.87(16) |
| 0.09 | ------ | 1.82(12) |
| 0.09 | ------ | 2.03(10) |

Table VII. Rates of Thermal Reaction of $3.10 \times 10^{-3}$ M $(DTN)W_2(CO)_{10}$ with Triisopropyl Phosphite in 1,2-Dichloroethane at 333.0 oK Monitored at 435 nm

| Ligand Conc. moles/liter | DTN Added moles/liter | $k_{obsd}$(step 1) $\times 10^{0}$ $sec^{-1}$ | $k'_{obsd}$(step 2) $\times 10^{1}$ $sec^{-1}$ |
|---|---|---|---|
| 0.6034 | ------ | 3.02(8) | 6.72(18) |
| 0.6020 | $3.10 \times 10^{-3}$ | 3.05(12) | 7.02(18) |

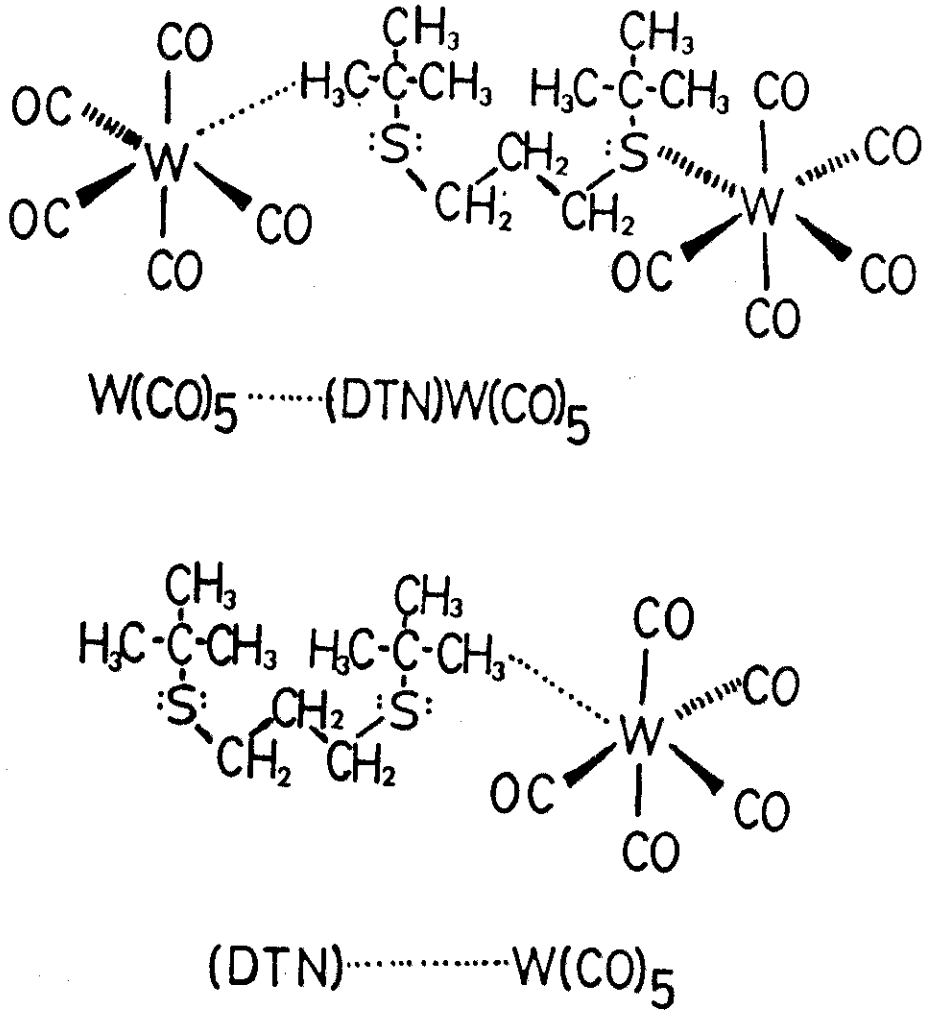


Figure 25. The behavior of DTN and $(DTN)W(CO)_5$ after their dissociation from $(DTN)W(CO)_5$ and $(DTN)W_2(CO)_{10}$.

reasonable when compared with those obtained by Wawersik and Basolo (5) for the reaction of $Mn_2(CO)_8(P(C_6H_5)_3)_2$ with $P(OC_6H_5)_3$ and $P(n\text{-}C_4H_9)_3$ (1/8.3 and 1/180 respectively). Nevertheless, most of the competition ratios determined in others' experiments range from 1/3 to 3. For example, (a) those in the piperidine substitution reaction of $Mo(CO)_5(C_6H_{11}N)$ complexes with the ligands $P(OCH_3)_3$, $P(C_6H_5)_3$, and $As(C_6H_5)_3$ performed by Covey and Brown (6) are near unity; (b) those in the substitution reactions of $(DTO)W(CO)_4$ with phosphorus-containing ligands such as $P(OCH_3)_3$, $P(OC_6H_5)_3$, and $P(C_6H_5)_3$ performed by Shultz and Dobson (7) vary from 0.5 to 2.5.

An explanation for the data listed in Table III is necessary. The data listed in Table III show that the values of competition ratios $k_{-1}/k_2$ and $k_{-3}/k_4$ are very close and the values of competition ratios $k_{-1}/k_2$ and $k_{-3}/k_4$ increases by increasing temperature. The largest value at 60.0 $^{o}C$ is nearly twice as large as the smallest one at 30.0 $^{o}C$. Based not only on these but also on the large value of $\Delta H^{\ddagger}$ for $k_{3d}$ listed in Table IV, one can suggest that the bulky coordinated DTN, $(DTN)W(CO)_5$, and ligand DTN remain in close vicinity to $W(CO)_5$, and can therefore easily react with $W(CO)_5$ complex to reform $(DTN)W_2(CO)_{10}$ for step 1 and form $(DTN)W(CO)_5$ for step 2 with an increase in temperature. The small negative value of $\Delta S^{\ddagger}$ for $k_{3d}$ listed in Table IV and the flash photolysis data listed in Table V and Table VI support this suggestion.

The flash photolysis data listed in Table VI show that $k_{obsd}$ for $W(CO)_5$(solvent) produced from the $(DTN)W_2(CO)_{10}$ complex is not influenced by adding various concentrations of triisopropyl phosphite. The values of decay rate constant k(= $dk_{obsd}/d[L]$) are close to zero. Since the value of $k^o_{obsd}$ for [L] = 0 listed in Table VI is approximately thirteen times larger than that of the average rate constant k' of $W(CO)_5$(solvent) produced from $W(CO)_6$ listed in Table V, one can understand why the values of rate constant k (= $dk_{obsd}/d[L]$) calculated for Table VI are close to zero based on the following equation (4-12):

$$K_{obsd} = k^o_{obsd} \text{ (for [L] = 0)} + k'[L] \quad \text{----------(4-12).}$$

One can conclude that the larger concentration ([L] = 0.09 M) of triisopropyl phosphite contributes much less in this decay reaction than the smaller concentration ($5 \times 10^{-4}$ M) of $(DTN)W(CO)_5$. This phenomenon results in the high values of competition ratios for step 1 and step 2 in this substitution reaction as shown in Table III.

Since the $k^o_{obsd}$ and k' in eq.(4-12) are the rate constants for the reactions of $W(CO)_5$(solvent) with $(DTN)W(CO)_5$ and $W(CO)_5$(solvent) with $P(OCH(CH_3)_2)_3$ respectively, the value of $k_{2f}/k'_{2f}$ (eq. 4-14 and 4-15) can be expressed as that of $k^o_{obsd}/k'$.

$$W(CO)_5(\text{solvent}) \underset{k_{-f}}{\overset{k_f}{\rightleftharpoons}} W(CO)_5 + \text{solvent} \quad \text{---------(4-13)}$$

$$W(CO)_5 + (DTN)W(CO)_5 \xrightarrow{k_{2f}} (DTN)W_2(CO)_{10} \text{ --------(4-14)}$$

$$W(CO)_5(solvent) \underset{k_{-f}}{\overset{k_f}{\rightleftharpoons}} W(CO)_5 + solvent \text{ ----------(4-13)}$$

$$W(CO)_5 + P(OCH(CH_3)_2)_3 \xrightarrow{k'_{2f}} P(OCH(CH_3)_2)_3W(CO)_5 \text{--(4-15)}$$

Thus, the value of competition ratio $k_{-1}/k_2$ for thermal reaction in mechanism I (Figure 20) can be calculated from flash photolysis data $k^o_{obsd}/k'$. From the data as shown in Table III, the value of competition ratio $k_{-1}/k_2$ (=13.11) calculated from $k^o_{obsd}/k'$ is consistent with those of $k_{-1}/k_2$ and $k_{-3}/k_4$ obtained from thermal reaction. The values of $k_{-1}/k_2$ and $k_{-3}/k_4$ are similar both at 30.0 $^oC$ and 60.0 $^oC$, and the values of $k_{-1}/k_2$ and $k_{-3}/k_4$ at 60.0 $^oC$ are twice larger than those of $k_{-1}/k_2$ and $k_{-3}/k_4$ at 30.0 $^oC$ respectively.

The values of $\Delta H^{\ddagger}$ and $\Delta S^{\ddagger}$ of a dissociative reaction are found to be positive. For the data of this experiment, the $\Delta H^{\ddagger}$ was 22.60 (1.41) kcal/mole and $\Delta S^{\ddagger}$ was -5.73 (4.44) e.u. for $k_{3d}$. The $\Delta S^{\ddagger}$ was small negative, which was probably due to attraction between the bulky ligand DTN and $W(CO)_5$ after dissociation. Similar results were published in another study in which the $\Delta S^{\ddagger}$ of a dissociative reaction of $(C_6H_5NH_2)W(CO)_5$ and $(C_6H_5)_3SbW(CO)_5$ were -6.4 e.u. and -4.8 e.u. respectively (8).

The W-S bond energies for the first and second dissociative steps are approximately equal; but the dissociative rate

constant of the first step, $k_{1d}$, is about four times as large as that of the second step, $k_{3d}$, at 60.0 °C. This can be explained in the following way:

Steric effect-- The first departing group ((DTN)$W(CO)_5$) is more bulky than the second departing group (DTN).

Statistical effect -- The triisopropyl phosphite can displace $W(CO)_5$ in (DTN)$W_2(CO)_{10}$ by breaking either of the W-S bonds in step 1; for step 2, there is only one W-S bond to be broken in (DTN)$W(CO)_5$.

All of the reasons above favor step 1, and strongly support the data as shown in Table II in which the dissociation of (DTN)$W(CO)_5$ from (DTN)$W_2(CO)_{10}$ is much favored over the dissociation of DTN from (DTN)$W(CO)_5$. In addition, these results indicate that the mechanism for step 1 (equation 1-21) suggested by Yang (1) is unreasonable because the value of $k_{1d}/k_{2d}$ (less than two) is too small.

The data of the plot of $1/k_{obsd}$ versus 1/[L] at 60.0 °C for step 1 are not as good as those for step 2, and data points in the plots of $1/k_{obsd}$ versus 1/[L] at 44.5 °C and 30.0 °C for step 1 are too scattered to permit determination of the rate constants. This scattering can be explained by the following reasons:

(a) From equations 2-1, 2-2, 2-3 and 2-4, the values of intercept $\ln\partial$ and slope ($-k_{obsd}$) in the plot of $\ln(A_t - A_\infty)$ versus time for step 1 depend on those of intercept r and slope ($-k'_{obsd}$) in the plot of $\ln(A_t - A_\infty)$ vs. time for

step 2, the small error of determination of $k'_{obsd}$ and r results in the large error of determination of $k_{obsd}$ especially under the condition that the value of $k_{obsd}$ and $k'_{obsd}$ are similar.

(b) From the data of $k_{obsd}$ and $k'_{obsd}$ at 60.0 $^{o}$C listed in Table I, the value of $k_{obsd}/k'_{obsd}$ (4-5) is less than that (5-10) for the reaction of $(DTN)W(CO)_4$ with $P(OCH_2)_3CCH_3$ (10), and much less than that (about 44) for the formation and decay of peroxonitrious acid HOONO (9).

The IR spectra for the reaction of $(DTN)W_2(CO)_{10}$ with triisopropyl phosphite in 1,2-dichloroethane as shown in Figure 26 can be used to study the change from $(DTN)W_2(CO)_{10}$ to $P(OCH(CH_3)_2)_3W(CO)_5$. The three main vibrational modes of $LW(CO)_5$ are $A_1^{(2)}$, E and $A_1^{(1)}$ (2). The $A_1^{(1)}$ and E modes are associated with the four equivalent CO groups, and the $A_1^{(1)}$ mode is that of the CO trans to L (11). From IR spectra as shown in Figure 26, one can understand that the vibrational modes $A_1^{(1)}$ (1903.8 $cm^{-1}$), E (1942.0 $cm^{-1}$) and $A_1^{(2)}$ (2073.6 $cm^{-1}$) of $(DTN)W(CO)_5$ complex or the $(DTN)W(CO)_5$ part of the $(DTN)W_2(CO)_{10}$ complex change to those $A_1^{(1)}$ (1900.1 $cm^{-1}$), E (1942.2 $cm^{-1}$) and $A_1^{(2)}$ (2076.0 $cm^{-1}$) of $P(OCH(CH_3)_2)_3W(CO)_5$.

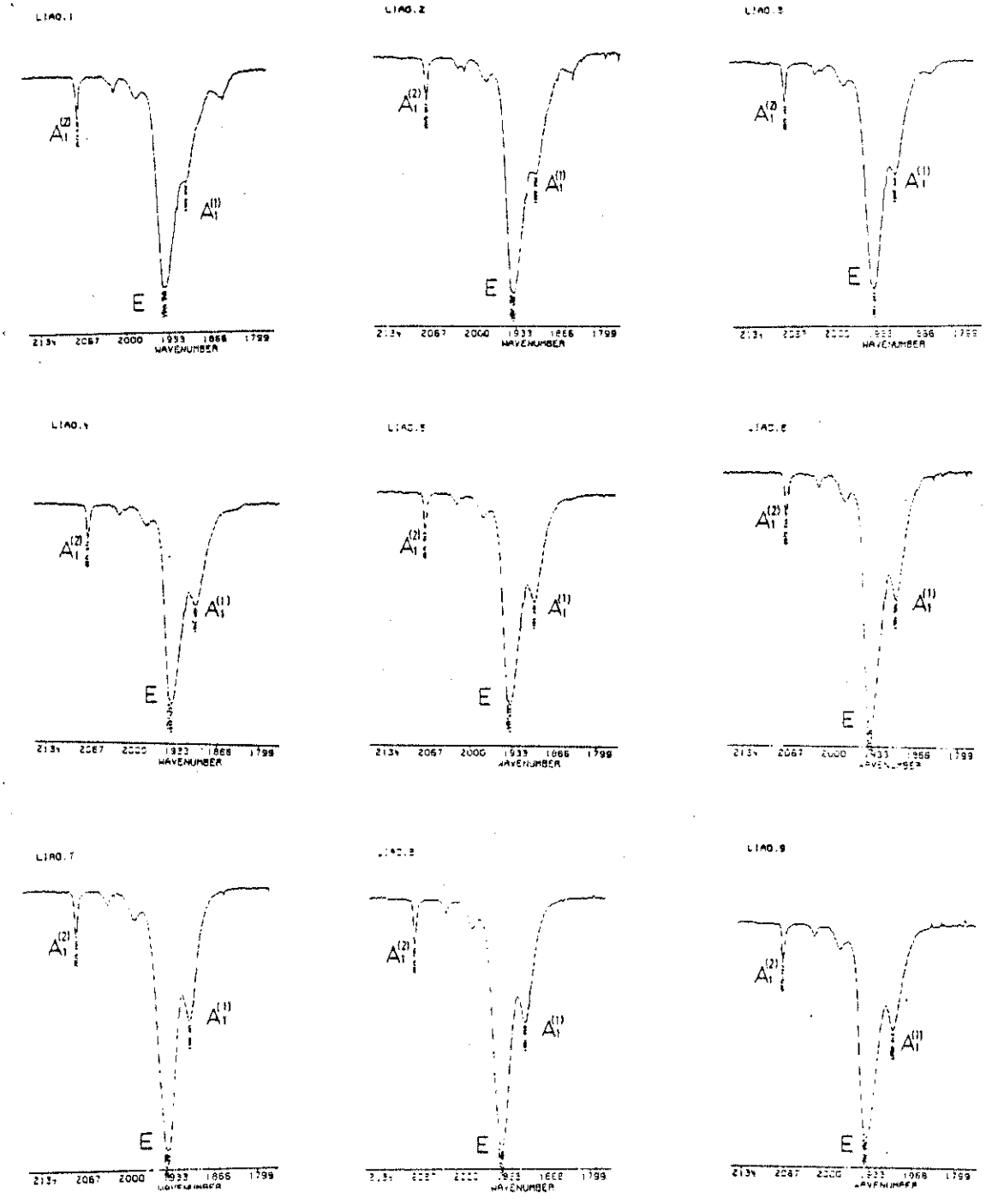


Figure 26. The infrared spectra for the reaction of $(DTN)W_2(CO)_{10}$ with triisopropyl phosphite in 1,2-dichloroethane at 333 °K.

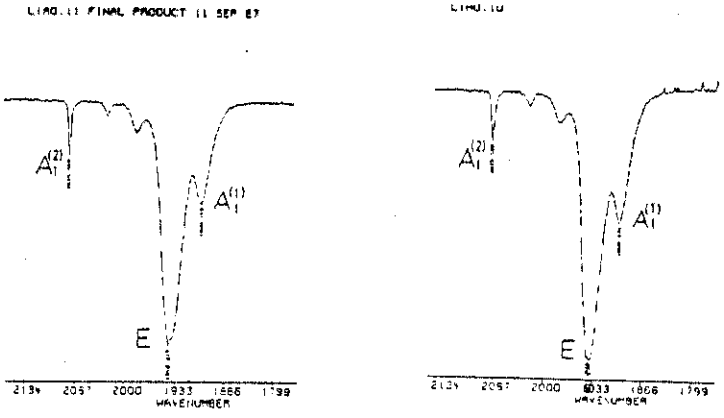


Figure 26. (continued)

## Chapter Bibliography

1. Yang, S. N. Masters Thesis, North Texas State University, 1982.

2. Angelici, R. J.; Malone, M. D. Inorg. Chem. 1967, 6, 1731.

3. Ingemanson, C. M.; Angelici, R. J. Inorg. Chem. 1968, 7, 2646.

4. Poilblanc, R.; Bigorgne, M. Bull. Soc. Chim. France. 1962, 1301.

5. Wawersik, H.; Basolo, F. Inorg. Chim. Acta, 1969, 3, 113.

6. Covey, W. D.; Brown, T. L. Inorg. Chem. 1973, 12, 2820.

7. Schultz, L. D.; Dobson, G. R. J. Organometal. Chem. 1976, 124, 19.

8. Dobson, G. R. Inorg. Chem. 1974, 13, 1790.

9. Espenson, J. H. Chemical Kinetics and Reaction Mechanism, McGraw Hill: New York; 1981, 22-24.

10. Dobson, G. R.; Schultz, L. D. J. Organometal. Chem. 1977, 131, 285.

BIBLIOGRAPHY


1. Angelici, R. J.; Basolo, F. J. Am. Chem. Soc. 1962, 84, 2495.

2. Angelici, R. J.; Malone, M. D. Inorg. Chem. 1967, 6, 1731.

3. Asali, K. J.; Basson, S. S.; Tucker, J. S.; Hester, B. C.; Cortes, J. E.; Awad, H. H.; Dobson, G. R. J. Am. Chem. Soc. 1987, 109, 5386-5392.

4. Covey, W. D.; Brown, T. L. Inorg. Chem. 1973, 12, 2820.

5. Darensbourg, D. J.; Darensbourg, M. Y. Inorg. Chem. 1970, 9, 1691.

6. Dobson, G. R. Inorg. Chem. 1974, 13, 1790.

7. Dobson, G. R.; Hodges, P. M.; Healy, M. A.; Poliakoff, M.; Turner, J. J.; Firth, S.; Asali, J. J. Am. Chem. Soc. 1987, 109, 4218-4224.

8. Dobson, G. R.; Schultz, L. D. J. Organometal. Chem. 1977, 131, 285.

9. Douglas, B. E.; McDaniel and Alexander, J. J. Concepts and Models of Inorgnic Chemistry, 2nd. Ed. Jon Wiley & Sons, Inc. New York, 1983, 329-363 and 404-416.

10. Espenson, J. H. Chemical Kinetics and Reaction Mechanism, McGraw Hill, New York, 1981, 22-24.

11. Graham, J. R.; Angelici, R. J. Inorg. Chem. 1967, 6, 2082.

12. Howell, J. A. S.; Burkinshaw, P. M. Chem. Rev. 1983, 83(5), 557.

13. Hyde, C. L.; Darensbourg, D. J. Inorg. Chem. 1973, 12, 1286.

14. Ingemanson, C. M.; Angelici, R. J. Inorg. Chem. 1968, 7, 2646.

15. Langford, C. H.; Gray, H. B. Ligand Substitution Processes, W. A. Benjamin, New York, N.Y., 1965, Chapter 1.

16. Linding, B. A.; Rodgers, M. A. J. J. Phys. Chem. 1979, 83, 1683.

17. Mitchell, P. R.; Parish, R. V. J. Chem. Educ. 1969, 46, 811.

18. Pardue, J. E.; Memering, M. N.; Dobson, G. R. J. Organometal. Chem. 1974, 71, 407

19. Poilblanc, R.; Bigorgne, M. Bull. Soc. Chim. France. 1962, 1301.

20. Purcell, K. F.; Kotz, J. C. Inorganic Chemistry, W. B. Saunders, Philadelphia, PA., 1979, 360-377.

21. Schultz, L. D.; Dobson, G. R. J. Organometal. Chem. 1976, 124, 19.

22. Sidgwick, N. V. The Chemical Elements and Their Compounds, Vols. I and II. New York, Oxford Univ. Press. 1950, 1703.

23. Wawersik, H.; Basolo, F. Inorg. Chim. Acta, 1969, 3, 113.

24. Werner, H.; Beck, W.; Englemann, H. Inorg. Chim. Acta, 1969, 3, 331.

25. Yang, S. N. "Kinetic Study of Ligand Exchange in μ-(2,2,8,8-tetramethyl-3,7-dithianonane)decarbonyl-ditungsten(0)," 1982, Masters Thesis, North Texas State University.